



RESEARCH ARTICLE

10.1029/2021GC010242

Origin and Age of Magmatism in the Northern Philippine Sea Basins

Key Points:

- Widely spread Eocene andesitic magmatism in northern Philippine Sea marks the onset of rifting in the Mesozoic arc terrane
- Late Eocene basalts in the Kita-Daito Basin could represent the last stage of spreading of the Kita-Daito Basin
- Rifting and spreading of the Mesozoic arc terrane in northern Philippine Sea postdate subduction initiation along the Izu-Bonin arc

Supporting Information:

Supporting Information may be found in the online version of this article.











Correspondence to:

O. Ishizuka,
o-ishizuka@aist.go.jp

Citation:

Ishizuka, O., Tani, K., Taylor, R. N., Umino, S., Sakamoto, I., Yokoyama, Y., et al. (2022). Origin and age of magmatism in the northern Philippine Sea basins. *Geochemistry, Geophysics, Geosystems*, 23, e2021GC010242. <https://doi.org/10.1029/2021GC010242>

Received 5 NOV 2021
Accepted 7 MAR 2022

Osamu Ishizuka^{1,2} , Kenichiro Tani³ , Rex N. Taylor⁴ , Susumu Umino⁵ , Izumi Sakamoto⁶, Yuka Yokoyama¹, Gen Shimoda¹ , Yumiko Harigane¹ , Yasuhiko Ohara^{2,7,8} , Chris E. Conway¹ , Americus Perez^{9,10} , and Shun Sekimoto¹¹ 

¹Geological Survey of Japan/AIST, Tsukuba, Japan, ²Japan Agency for Marine-Earth Science and Technology, Yokosuka, Japan, ³Department of Geology and Paleontology, National Museum of Nature and Science, Tsukuba-shi, Japan, ⁴School of Ocean and Earth Sciences, University of Southampton, Waterfront Campus, Southampton, UK, ⁵Division of Natural System, Kanazawa University, Kanazawa, Japan, ⁶School of Marine Science and Technology, Tokai University, Shimizu, Japan, ⁷Ocean Research Laboratory, Hydrographic and Oceanographic Department of Japan, Tokyo, Japan, ⁸Department of Earth and Planetary Sciences, Nagoya University, Nagoya, Japan, ⁹Guangzhou Institute of Geochemistry, The Chinese Academy of Sciences, Guangzhou, The People's Republic of China, ¹⁰Department of Science and Technology, Philippine Nuclear Research Institute, Quezon City, Philippines, ¹¹Institute for Integrated Radiation and Nuclear Science, Kyoto University, Kumatori, Japan

Abstract A Robust tectonic reconstruction of the Philippine Sea Plate around ~52 Ma is a prerequisite in understanding the process of subduction initiation and establishment of the Izu-Bonin-Mariana arc. This study investigates origins and timing of basin formation in the still poorly understood oldest part of the northern Philippine Sea plate. We have established that andesitic magmatism in the form of the Northern Philippine Sea volcanics is widely distributed across this area. It is founded on both a Mesozoic arc terrane (Daito Ridge Group) and an intervening basin (Kita-Daito Basin). Their narrow Eocene age range (45–41 Ma) and lack of systematic spatial variation in geochemistry implies that this magmatism was not associated with on-going subduction, but related to the rifting/spreading event forming the Kita-Daito Basin. The arc-like geochemistry of the volcanics seems to indicate melting of lithospheric mantle which had been previously metasomatized by Mesozoic subduction of a plate with Pacific-MORB isotopic characteristics. Late Eocene basaltic magmatism also found in the Kita-Daito Basin does not have arc-like characteristics, and could have formed from low-degree melts of asthenospheric mantle associated with the final stage of Kita-Daito Basin spreading. As onset of activity of the Northern Philippine Sea volcanics is essentially synchronous with the magmatism associated with the Oki-Daito mantle plume, it is possible that both magmatism and rifting of the Kita-Daito Basin were triggered by the arrival of the Oki-Daito mantle plume in this region. These results demonstrate that the Kita-Daito Basin postdates subduction initiation of the Pacific Plate along the Izu-Bonin-Mariana arc.

Plain Language Summary This study investigates origin and age of ocean basins in the still poorly understood northern Philippine Sea plate. This area will help us appreciate what happens during the initiation of a new destructive plate margin. We recovered rock samples from the Northern Philippine Sea Seamounts and Kita-Daito Basin, and determined their age and composition. These volcanoes were active between 45 and 41 Ma and are found widely distributed across the older crust of the northernmost Philippine Sea Plate. Despite the geographical spread of these volcanoes, they have a similar composition across the region. This indicates they were produced during stretching of the older crust, which reactivated the older underlying upper mantle. A possible reason for this stretching may have been the impact of a mantle plume beneath this region.

1. Introduction

Hypotheses proposed for the initiating a destructive plate margin include spontaneous subduction or induced nucleation (e.g., Stern, 2004). These competing models can be tested by reconstruction of the volcanic systems which lay astride the western Pacific margin at around 52 Ma during the process of subduction initiation. Since gravitational instability between the neighboring plates is thought to be a critical factor for subduction initiation (e.g., Leng & Gurnis, 2015), it is important to understand the age, origin and crustal structure of the overriding plate.

© 2022. The Authors.

This is an open access article under the terms of the [Creative Commons Attribution License](https://creativecommons.org/licenses/by/4.0/), which permits use, distribution and reproduction in any medium, provided the original work is properly cited.

In addition to these hypotheses for subduction initiation, recently role of mantle plume in initiation of plate subduction has been discussed (e.g., Gerya et al., 2015; van Hinsbergen et al., 2021; Whattam & Stern, 2015). Focused magmatic weakening and thinning of lithosphere above the plume is regarded as one of the key physical factors to trigger subduction initiation combined with strong negative buoyancy of the oceanic lithosphere and lubrication of slab interface (Gerya et al., 2015). In this context, understanding mechanism of subduction initiation along the Pacific margin beneath the Philippine Sea Plate requires precise knowledge about tectonic and magmatic events around the time of subduction initiation. Interplay between plate subduction, seafloor spreading and plume impact on the Philippine Sea Plate needs to be understood.

It is recognized that in the Eocene the Philippine Sea Plate experienced significant tectonic and magmatic events in addition to subduction initiation along the margin with the Pacific Plate.

Ocean Island basalt (OIB) volcanism commenced at around 50 Ma, possibly associated with arrival of the Oki-Daito plume (Ishizuka et al., 2013). This volcanism formed oceanic plateaus including Oki-Daito Rise, Urdaneta Plateau and Benham Rise as well as small volcanoes on the Oki-Daito Ridge and sills in the Minami-Daito Basin (Figure 1a: Hickey-Vargas, 1998; Ishizuka et al., 2013).

Another major Eocene event affecting the Philippine Sea plate was the opening of the West Philippine Basin (Figure 1a). Onset of spreading of the basin is estimated to be around 55 Ma, but no direct dating of the ocean crust of the oldest part of the basin has been made, and a robust interpretation of seafloor magnetic anomalies is not available (Deschamps & Lallemand, 2002). Also, the exact tectonic setting and mechanism of spreading in the West Philippine Basin is still a matter of debate (e.g., Deschamps & Lallemand, 2002).

Most of the previous tectonic models of the Philippine Sea Plate assumed that the Daito Ridge Group and intervening basins existed prior to the Eocene in the same form they are now (Deschamps & Lallemand, 2002; Hall, 2002), that is, the basins formed prior to subduction initiation of the Izu-Bonin-Mariana (IBM) arc.

Recent expedition of International Ocean Discovery Program (IODP) Exp. 351 (Site U1438: Figures 1a–1c) recovered ocean crust of the Amami-Sankaku Basin (Figure 1) just east to the Amami Plateau of the Daito Ridge Group (Figure 1), and provided new evidence for the age of the basins in the northernmost Philippine Sea Plate (Arculus et al., 2015; Ishizuka et al., 2018). Contrary to the hypothesis prior to drilling that the age of the Amami Sankaku Basin is similar to that of the Daito Ridge Group, that is, Mesozoic, it was found that the basin formed in the Eocene (49 Ma), following the subduction initiation of the IBM arc. This seems to raise the possibility that the basins intervening the Daito Ridge Group may be also younger than previously expected. Recently Lallemand (2016) proposed that these basins might have formed as a consequence of spreading perpendicular to the newly born IBM arc subduction zone based on some early results of IODP Exp. 351 and compilation of reported data.

Accordingly, there are still multiple tectonic and magmatic events on the Philippine Sea Plate with no robust age constraints and unclear temporal relationships. These events may or may not be associated with subduction initiation along the Philippine Sea Plate margin. In this study we have investigated magmatism in the oldest part of the Philippine Sea Plate to (a) reveal for the first time the age and origin of Kita-Daito Basin and the intervening Daito Ridge Group; (b) understand origin of Eocene magmatism widely distributed in and around the Daito Ridge Group. The outcome of these studies will assist in understanding the time sequence of magmatic and tectonic events which took place within a relatively short period around 45–52 Ma, that is, during and after subduction initiation along the Pacific margin.

2. Geological Background

2.1. Daito Ridge Group

The Daito Ridge Group is a complex array of ridges and basins (Figure 1c). It comprises three remnant arcs: the Amami Plateau, the Daito and Oki-Daito Ridges, and two ocean basins neighboring these ridges (the Kita-Daito and Minami-Daito Basins). Granites and other volcanics of Cretaceous age (e.g., Hickey-Vargas, 2005; Matsuda et al., 1975; Tani et al., 2012) have been reported from the Amami Plateau, which is estimated to have a maximum of 17–18 km thick crust (Nishizawa et al., 2014). This Cretaceous magmatism shows a geochemical affinity with arc rocks, which implies that the main part of Amami plateau crust formed by Cretaceous subduction zone magmatism (Hickey-Vargas, 2005).

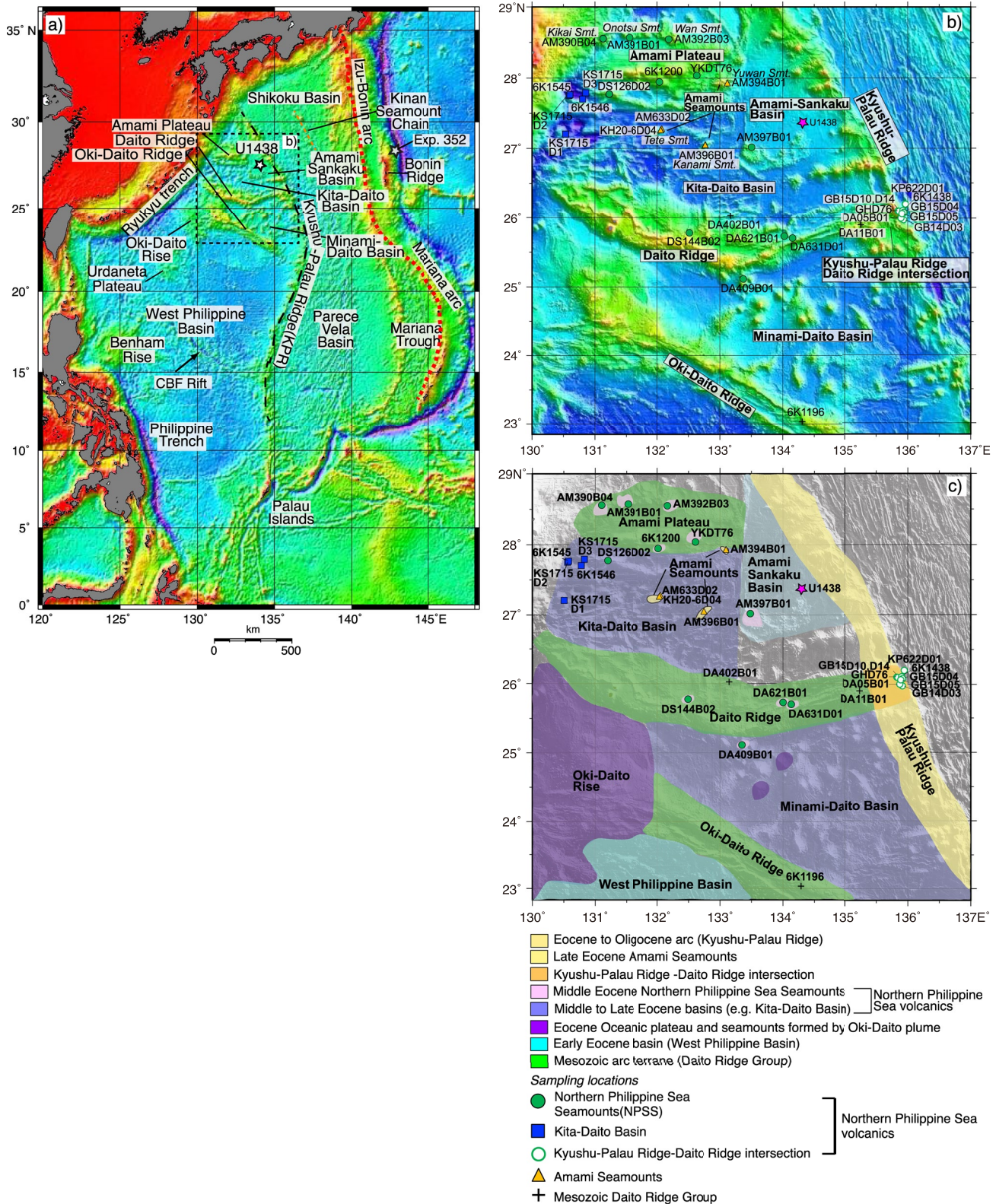


Figure 1. (a) Overview of the bathymetry of the Philippine Sea Plate and location of the studied area, (b) Detailed bathymetric map of the studied area. Locations of submarine sampling stations are shown with the symbols used in the geochemical plots. Station names in parentheses mean that the data have been published in Ishizuka, Taylor, et al. (2011). (c) Schematic tectonic map of the studied area. Age information is based on results of this study and previous studies (e.g., Deschamps & Lallemand, 2002; Ishizuka, Taylor, et al., 2011, 2013, 2018).

Daito Ridge, to the south of the Amami Plateau, is generally east–west trending and intersects the Kyushu–Palau Ridge (KPR) at its eastern end (Figures 1b and 1c). Low-grade metamorphic rocks, volcanic rocks, serpentinized peridotite and some sedimentary rocks were recovered by dredging, drilling and submersible survey, apparently from beneath an Eocene sedimentary cover (Ishizuka, Taylor, et al., 2011; Mizuno et al., 1975, 1978; Morishita et al., 2018; Yuasa & Watanabe, 1977). Two of the drilled andesites, with the distinctive trace element characteristics of arc magmas, yielded $^{40}\text{Ar}/^{39}\text{Ar}$ ages of 116.9 and 118.9 Ma (Ishizuka, Taylor, et al., 2011). Morishita et al. (2018) argued based on trace element characteristics of the minerals from the peridotite that the Daito Ridge peridotites had been enriched with slab-derived components and belong to an exhumed mantle section of a remnant proto-Philippine Sea island arc. These results indicate that the Daito Ridge is an exposed remnant arc terrane produced above a Mesozoic subduction zone.

Nishizawa et al. (2014) showed that the crustal thickness of the Daito Ridge varies between 13 and 20 km. In the western part of the ridge the crust is generally thinner in the north compared to the south, while in the eastern ridge, with a narrow bathymetric high, the crustal thickness is the same north and south. Nishizawa et al. (2014) also mentioned that a notable feature of the Daito Ridge crust is that a material with $V_p \leq 6.3$ km/s and a thickness of 6–11 km is concentrated in the southern part, while a material with $V_p \geq 6.3$ km/s ascends closer to the seafloor toward the Kita-Daito Basin in the north.

The Oki-Daito Ridge (Figure 1) is a ~600 km-long, WNW–ESE trending ridge, which forms the margin of the Minami-Daito Basin to the north, and bounds the West Philippine Basin to the south. This ridge is characterized by development of extensive escarpments, troughs, and lineaments dominantly in NW–SE direction (Figure 1b). Eocene limestone and tuff as well as basaltic to andesitic volcanic rocks were reported from the Oki-Daito Ridge (Mizuno et al., 1975; Shiki et al., 1985), implying that the crust formed prior to Eocene and has a similar Mesozoic arc origin to the Amami Plateau and Daito Ridge.

The Oki-Daito Rise is a wide bathymetric high to the west of the Oki-Daito Ridge, which occupies an area of ~200 km². The eastern margin of the rise appears to overlap the western part of the Oki-Daito Ridge. The rise exposes basalts with Ocean-Island Basalt (OIB)–like geochemical characteristics with an age range between 40 and 44 Ma (Ishizuka et al., 2013). Ishizuka et al. (2013) proposed that the rise formed by magmatism caused by arrival of Oki-Daito plume, implying different origin to the Oki-Daito Ridge.

The crustal structure of the Oki-Daito Ridge is characterized by the presence of a thick middle crust with V_p of 6.3–6.8 km/s beneath the bathymetric high (Nishizawa et al., 2014). The upper crust (with V_p of approximately 3.0–6.3 km/s) is slightly thicker beneath the valley. The thickness of the lower crust (with V_p of 6.8–7.2 km/s) is 7–10 km, and the total crustal thickness is 20–30 km. The Oki-Daito Rise is characterized by much thinner crust (10–15 km) compared to the neighboring Oki-Daito Ridge.

2.2. Basins in the Daito Ridge Group

Daito Ridge Group has intervening oceanic basins such as Kita-Daito Basin, Minami-Daito Basin and Amami Sankaku Basin and neighboring West Philippine Basin.

The Kita-Daito Basin separates the Amami Plateau and the Daito Ridge. No rock sampling has been reported from this basin to constrain its age and origin. The V_p model of the Kita-Daito Basin suggests the presence of a 4–6 km thick crust, similar to the backarc basin oceanic crust in the Shikoku and Parece Vela Basins, as revealed by Nishizawa et al. (2011, 2014). They also imply that roughly east-west aligned magnetic anomalies in the Kita-Daito Basin might have been produced by extension and seafloor spreading in the north-south direction (Nishizawa et al., 2014). By contrast, Kasuga et al. (1986) interpreted that these lineations are related to topographic relief.

The Minami-Daito Basin, located between the Daito and Oki-Daito Ridges, has abundant bathymetric highs in the basin (Figure 1). Deep Sea Drilling Project (DSDP) at Site 446 in the western part of the basin and shallow drilling at a seamount in the basin recovered basalts which clearly have OIB–like geochemical characteristics, and show $^{40}\text{Ar}/^{39}\text{Ar}$ ages of 43–51 Ma (Hickey-Vargas, 1998; Ishizuka et al., 2013). Nishizawa et al. (2016) showed that the Minami-Daito Basin has thick crust of around 10 km and high P_n velocity of 8.1–8.3 km/s, which is notably different from a typical oceanic crust.

Amami Sankaku Basin is an oceanic basin between the KPR to the east and the Amami Plateau and the Kita-Daito Basin to the west (Figure 1). This means that the basin corresponds to the reararc area of the KPR, that is, reararc of ancient Izu-Bonin-Mariana arc. IODP Exp.351 recovered igneous basement of this basin, which consists of basaltic lava flows (Arculus et al., 2015). These basalts are geochemically MORB-like, and give ages of 49 Ma (Hickey-Vargas et al., 2018; Ishizuka et al., 2018; Yogodzinski et al., 2018). As such, they have a similar age and geochemistry to forearc basalts (FAB; Reagan et al., 2010; Ishizuka, Tani, et al., 2011) which are associated with seafloor spreading at subduction initiation. Hence the Amami Sankaku Basin basalts are interpreted to have a similar origin (Hickey-Vargas et al., 2018; Ishizuka et al., 2018; Yogodzinski et al., 2018). The igneous crust flooring the Amami Sankaku Basin is estimated to have normal oceanic crust of about 6 km thick (Assuming a V_p 6 km/S).

The West Philippine Basin is an ocean basin occupying the western half of the Philippine Sea plate and is bounded to the north by the Oki-Daito Ridge (Figure 1a). Deschamps and Lallemand (2002) proposed that the opening of the West Philippine Basin initiated at 55 Ma as a backarc rifting/spreading of subduction along the paleo-Philippine arc. The spreading axis was parallel to the paleo-Philippine arc but became inactive when a new spreading ridge, from which the major part of the West Philippine Basin formed, propagated from the eastern part of the basin. However, interpretation of magnetic anomaly of the northernmost part of the basin, which is supposed to be the oldest part of the basin, is highly questionable (Deschamps & Lallemand, 2002), and no reliable age constraints have been obtained from this part of the basin. Major stage of the spreading appears to have ceased at around 35 Ma (Sasaki et al., 2014).

2.3. Kyushu-Palau Ridge (KPR)-Daito Ridge Intersection

The KPR extends continuously over a distance of ~2,600 km from Kyushu to the Palau Islands (Figure 1). This ridge is a remnant arc structure, which was separated from the main IBM arc by spreading of the Shikoku and Parece Vela Basins (e.g., Karig, 1975; Ishizuka, Taylor, et al., 2011). The spreading is estimated to have initiated by c. 25 Ma, at which point the volcanism along the KPR appears to have ceased (Arculus et al., 2015; Brandl et al., 2017; Ishizuka, Taylor, et al., 2011; Johnson et al., 2021; McCarthy et al., 2021). Accordingly, the KPR is expected to record arc volcanism from its inception at c. 52 Ma until around 25 Ma. KPR and Daito Ridge intersect at around 26°N (Figures 1b and 1c). Volcanic and plutonic rocks recovered from this area are 43–48 Ma (Ishizuka, Taylor, et al., 2011). These ages are significantly younger than the Jurassic-Cretaceous ages obtained from Daito Ridge itself (116–119 Ma; Ishizuka, Taylor, et al., 2011; Tani et al., 2012). As with other parts of the KPR, these intersection volcanics have the geochemical characteristics of arc magmatism (Ishizuka, Taylor, et al., 2011). Since the Daito Ridge formed in the Cretaceous and is overlain by middle Eocene shallow marine sediment (Mizuno et al., 1978), volcanism at the KPR–Daito Ridge intersection is likely to have occurred in shallow water or subaerially on the Daito Ridge.

3. Sample Studied

Samples studied here were collected by (a) drilling using the Deep-sea Boring Machine System (BMS) fitted to R/V *Hakurei-maru No.2*, (b) dredge sampling conducted by R/V *Hakurei-maru No.2*, R/V *Shinsei maru*, R/V *Hakuho maru* and R/V *Bosei-maru*, (c) diving survey using submersible “*Shinkai 6500*” equipped with 2 manipulators (Figure 1b). Brief descriptions of the sample material including the recovery method are listed in Table S1 in Supporting Information S1). Drilling was normally conducted on flat sediment-covered ridge tops and seamounts or on gentle slopes (less than 10°). Depth of drilling penetration was normally 5–10 m. Dredge sampling and diving surveys were conducted at steep escarpments. Imaging of sampling locations (sampling track in case of dredging) were made for all the sampling stations except for the dredging at KPR–Daito Ridge intersection.

3.1. Kita-Daito Basin

Volcanics collected from the Kita-Daito Basin are mostly plagioclase-phyric andesite with subordinate amount of clinopyroxene and orthopyroxene phenocrysts. Fresh material has mostly intact both phenocrysts and groundmass, while strongly altered samples show pervasive replacement by chlorite, epidote, and occasional clays. Only fresh samples were analyzed and reported here. These samples were recovered by dredging (KS1715 cruise) and

Shinkai 6500 submersible diving survey (Figure 1b: Dives 6K1545 and 6K1546). Since the submersible diving surveyed the deepest section of the Kita-Daito Basin, the andesites are thought to represent the Kita-Daito Basin crust.

3.2. Northern Philippine Sea Seamounts

Seamounts whose ages and geochemical characteristics remain unknown distribute in the Daito Ridge Group area. We collectively call these seamounts as Northern Philippine Sea Seamounts. Northern Philippine Sea Seamounts are characterized by occurrence of andesite with hornblende phenocrysts (Figure 1b: DS144B02, AM390B04 (Kikai Seamount), AM391B04 (Onotsu Seamount), AM392B03 (Wan Seamount), DA631D01, 6K1200). Some samples from 6K1200 contain xenoliths of metamorphosed sedimentary rocks, which are thought to have come from Amami Plateau crust, which provides the basement for the volcano which Dive 6K1200 investigated. These andesites form volcanic edifices that are constructed upon the Amami Plateau and the Daito Ridge.

3.3. KPR–Daito Ridge Intersection

Volcanic rocks and plutonic rocks were recovered from the KPR–Daito Ridge intersection. Basaltic to andesitic volcanic rocks were recovered from 3 sites (Figure 1b: DA05B01, KP622D01, GB14D03), and andesites from GB14D03 show porphyritic texture with abundant plagioclase. Plutonic rocks were recovered from multiple locations. Based on diving observations, these plutonic rocks were widely exposed along the escarpment facing Shikoku Basin, which are thought to have formed during the initiation of rifting along the Izu-Bonin arc to form the Shikoku Basin. Tonalitic to dioritic rocks were recovered from dredge sites GHD76, GB15D05, GB15D10 and GB15D14, and Dive 6K1438 (Figure 1b). These diorites contain amphiboles, both with or without biotite. Gabbroic rocks were collected from GB15D04 and D14, and Dive 6K1438 (Figure 1b).

3.4. Amami Seamounts

Three seamounts in the Kita-Daito Basin (Amami Seamounts hereafter) returned distinct rocks from other sampling stations in the area (Figure 1b). A NE-SW-elongated seamount with more than 2,000 m height in the central part of the basin (Kanami Seamount: AM396B01), and an ENE-WSW-elongated seamount with similar height near the northern margin of the basin (Yuwan Seamount: AM394B01) were drilled, and both sites returned slightly vesiculated, sparsely phyric olivine basalts. Drilling at another seamount WNW of AM396B01, with relative height of around 1,400 m, recovered pillow lava blocks of olivine basalt with abundant plagioclase phenocrysts (Tete Seamount: AM633D02). Dredge sampling at the same seamount recovered basalt lava blocks with fresh glass rind (KH20-6D04).

3.5. Daito and Oki-Daito Ridges

Volcanic rocks were recovered that are thought to represent the main crustal construction of the Daito and Oki-Daito Ridges (Figure 1b). Hence, this material is expected to provide information about age and geochemical characteristics of volcanism associated with formation of the Daito Ridge Group. Samples include aphyric basalt (DA11B01), clinopyroxene-olivine basalt (DA402B01) and two pyroxene porphyritic andesite (6K1196 samples from Dive 6K1196).

4. Analytical Procedures

4.1. $^{40}\text{Ar}/^{39}\text{Ar}$ Dating

Ages of the fresh volcanic rocks were determined using the $^{40}\text{Ar}/^{39}\text{Ar}$ dating facility at the Geological Survey of Japan/AIST. Details of the procedures are reported in Ishizuka et al. (2009, 2018). 10–15 mg of phenocryst-free groundmass, crushed and sieved to 250–500 μm in size, was analyzed using a stepwise heating procedure. The samples were treated in 6N HCl for 30 min at 95°C with stirring to remove any alteration products (clays and carbonates) present in interstitial spaces. After this treatment, samples were examined under a microscope. In case of dioritic samples, biotite crystals were separated by tapping and hand-picking from the sieved 250–500 μm fractions. Biotite separates were used for analysis without acid leaching. Sample irradiation was done either at

(a) the JMTR, JRR3 and JRR4 reactors, (b) the Kyoto University Reactor (KUR), (c) the CLICIT facility of the Oregon State University TRIGA reactor. At the KUR, the neutron irradiation was performed for 10 hr at the hydro-irradiation port under 1 MW operation, where thermal and fast neutron fluxes are 1.6×10^{13} and 7.8×10^{12} n/cm² s, respectively, or for 2 hr under 5 MW operation, where thermal and fast neutron fluxes are 8.15×10^{13} and 3.93×10^{13} n/cm² s respectively.

Sanidine separated from the Fish Canyon Tuff (FC3) was used as flux monitor and assigned an age of 27.5 Ma, which has been determined against the primary standard for our K-Ar laboratory, Sori biotite, the age of which is 91.2 Ma (Uchiumi & Shibata, 1980).

A continuous Ar ion laser (Coherent INNOVA310: for analysis No. U05xxx and U06xxx) and CO₂ laser (NEWWAVE MIR10-30: for the rest of the analyses) were used for sample heating. For the CO₂ laser heating system, a faceted lens was used to obtain a 3.2 mm-diameter beam with homogenous energy distribution to ensure uniform heating of the samples during stepwise heating analysis. Argon isotopes were measured in a peak-jumping mode on a VG Isotech VG3600 noble gas mass spectrometer fitted with a BALZERS electron multiplier for analysis No. U05xxx, U06xxx, U08xxx, U10xxx and U11xxx, and on an IsotopX NGX noble gas mass spectrometer fitted with a Hamamatsu Photonics R4146 secondary electron multiplier for analysis No. U17xxx, U18xxx, U19xxx, U20xxx and U21xxx.

Correction for interfering isotopes was achieved by analyses of CaF₂ and KFeSiO₄ glasses irradiated with the samples. The blank of the system including the mass spectrometer and the extraction line was 7.5×10^{-14} ml STP for ³⁶Ar, 2.5×10^{-13} ml STP for ³⁷Ar, 2.5×10^{-13} ml STP for ³⁸Ar, 1.0×10^{-12} ml STP for ³⁹Ar and 2.5×10^{-12} ml STP for ⁴⁰Ar with the VG3600 instrument, and 2.9×10^{-14} ml STP for ³⁶Ar, 1.4×10^{-13} ml STP for ³⁷Ar, 1.0×10^{-14} ml STP for ³⁸Ar, 1.2×10^{-14} ml STP for ³⁹Ar and 1.9×10^{-12} ml STP for ⁴⁰Ar with the NGX mass spectrometer. Blank analyses were done every 2 or 3 step analyses. All errors for ⁴⁰Ar/³⁹Ar results are reported at one standard deviation. Errors for ages include analytical uncertainties for Ar isotope analysis, correction for interfering isotopes, and J value estimation. An error of 0.5% was assigned to J values as a pooled estimate during the course of this study. Results of Ar isotopic analyses and correction factors for interfering isotopes are presented in the supplementary data (Table S2 in Supporting Information S1).

Plateau ages were calculated as weighted means of ages of plateau-forming steps, where each age was weighted by the inverse of its variance. The age plateaus were determined following the definition by Fleck et al. (1977), but in some cases we adopted ages from steps which do not strictly satisfy the definition with reasonings detailed in Results section. Inverse isochrons were calculated using York's least squares fit, which accommodates errors in both ratios and correlations of errors (York, 1969).

4.2. Zircon U-Pb Dating

After careful cleaning of the samples by ultrasonic washing machine, 100–400 g of sample slabs were crushed by the selective fragmentation device using high-voltage pulsed electric discharges (selFrag-Lab) installed in the National Museum of Nature and Science (NMNS) to maximize the yield of zircon recovery. The heavy minerals were concentrated by panning and further processed with a hand magnet, and the remaining fractions were purified using heavy liquid (diiodomethane) separation.

Zircon grains from the samples, the zircon standard TEMORA-2 (417 Ma; Black et al., 2004), OD-3 (33 Ma; Iwano et al., 2013) and the glass standard NIST SRM610 were mounted in an epoxy resin and polished down to grain centers. Both the backscattered electron and cathodoluminescence (CL) images were obtained using a scanning electron microscope (JEOL JSM-6610) at NMNS to select the sites for analysis. In order to determine crystallization age of the zircons, grain rims free of inclusions were selected for analysis.

The U-Pb dating was undertaken using laser ablation inductively coupled plasma mass spectrometry system (LA-ICP-MS) at the NMNS in Japan, with the NWR213 laser ablation system (Electro Scientific Industries) in conjunction with the Agilent 7700x quadrupole ICP-MS (Agilent Technologies). The experimental conditions and the procedures followed for the measurements were based on Tsutsumi et al. (2012). U and Th concentrations were calibrated by using ²⁹Si as an internal calibrant and NIST SRM610 standard glass as the reference material. Pb isotope ratios (²⁰⁷Pb/²⁰⁶Pb and ²⁰⁸Pb/²⁰⁶Pb) are also calibrated using NIST SRM610 as reference material. ²⁰⁶Pb/²³⁸U ratios are calibrated using TEMORA-2 standard zircon. The spot size of the laser

was approximately 25 μm . A correction for common Pb was made on the basis of the measured ^{207}Pb (^{207}Pb correction) or ^{208}Pb and Th/U ratio (^{208}Pb correction) (e.g., Williams, 1998) and the model for common Pb compositions proposed by Stacey and Kramers (1975). Tera-Wasserburg concordia diagrams were constructed using the ^{208}Pb -corrected $^{207}\text{Pb}^*/^{206}\text{Pb}^*$ and $^{238}\text{U}/^{206}\text{Pb}^*$ ratios, and ^{207}Pb -corrected $^{206}\text{Pb}^*/^{238}\text{U}$ ages were used to calculate weighted means (Williams, 1998). $^{207}\text{Pb}^*$ and $^{206}\text{Pb}^*$ indicate radiometric ^{207}Pb and ^{206}Pb , respectively. IsoplotR program (Vermeesch, 2018) were used to construct the Tera-Wasserburg Concordia diagrams and to calculate the weighted mean ages. The uncertainties in the mean ^{238}U - $^{206}\text{Pb}^*$ ages represent 95% confidence intervals (95% conf.). The data of secondary standard OD-3 zircon obtained during analysis yielded a weighted mean age of 32.39 ± 0.32 Ma (Table S3 in Supporting Information S1: 95% conf.; $n = 35$; MSWD = 1.12), concordant with the previously reported ID-TIMS age of 32.853 ± 0.016 Ma (Lukács et al., 2015).

4.3. Whole Rock Chemistry

About 20 g of rock chips were ultrasonically cleaned with distilled water, and then crushed with an iron pestle and pulverized using an agate mortar. Whole rock major elements were analyzed on glass beads, prepared by fusing 1:10 mixtures of 0.5 g subsamples and lithium tetraborate. The glass beads were analyzed using a Panalytical Axios XRF spectrometer at the Geological Survey of Japan/AIST. External uncertainty and accuracy are generally <2% (2.s.d), but Na could have as much as ~7% analytical uncertainty. The data for each element are in agreement with accepted values and uncertainties of international standards (Table S4 in Supporting Information S1).

The rare-earth elements (REE), V, Cr, Ni, Rb, Sr, Y, Zr, Nb, Cs, Ba, Hf, Ta, Pb, Th and U concentrations were analyzed by ICP-MS on a VG Platform instrument and Agilent 7900, both at the Geological Survey of Japan/AIST. About 100 mg of powder from each sample was dissolved in a HF-HNO₃ mixture (5:1) using screw-top Teflon beakers. In case of digestion of felsic plutonic rocks, digestion using microwave dissolution system was applied (Anton Paar Mutiwave 3000). After evaporation to dryness, the residues were re-dissolved with 2% HNO₃ prior to analysis. In and Re were used as internal standards, while JB2 with a similar level of dilution to the samples was used as an external standard during ICP-MS measurements. Instrument calibration was performed using 5–6 calibration solutions made from international rock standard materials (including BIR-1, BCR-1, AGV-1, JB1a, BEN). Reproducibility is generally better than $\pm 4\%$ (RSD) for the REE, and better than $\pm 6\%$ (RSD) for other elements except those with very low concentration and Ni (see BHVO2 analysis in Table S4 in Supporting Information S1). Detection limits vary from element to element, but for elements with low concentrations, such as REE and Ta, limits typically fall within a range from 0.2 to 2 pg g^{-1} .

4.4. Radiogenic Isotopic Composition

Isotopic compositions of Sr, Nd, and Pb were determined on 500 mg of hand-picked 0.5–1 mm rock chips. The chips were leached in 6M HCl at 140°C for 20–30 min prior to dissolution in HF-HNO₃. Sr, Nd and Pb isotope ratios were measured on a nine-collector VG Sector 54 mass spectrometer. Sr was isolated using Sr resin (Eichrom Industries, Illinois, USA). For Nd isotopic analysis, the REE were initially separated by cation exchange, before isolating Nd on Ln resin (Eichrom Industries, Illinois, USA) columns. Procedural Sr and Nd blanks were considered negligible relative to the amount of sample analyzed. Sr and Nd isotopic compositions were determined as the average of 150 ratios by measuring ion beam intensities in multi-dynamic collection mode. Isotope ratios were normalized to $^{86}\text{Sr}/^{88}\text{Sr} = 0.1194$ and $^{146}\text{Nd}/^{144}\text{Nd} = 0.7219$. Measured values for NBS SRM-987 and JNdi-1 (Tanaka et al., 2000) were $^{87}\text{Sr}/^{86}\text{Sr} = 0.710278 \pm 19$ (2 s.d., $n = 33$) and $^{143}\text{Nd}/^{144}\text{Nd} = 0.512104 \pm 10$ (2 s.d., $n = 38$) during the measurement period. All $^{87}\text{Sr}/^{86}\text{Sr}$ ratios were normalized to NBS SRM-987 $^{87}\text{Sr}/^{86}\text{Sr} = 0.710248$ (Thirlwall, 1991), and $^{143}\text{Nd}/^{144}\text{Nd}$ ratios were normalized to JNdi-1 = 0.512115 (Tanaka et al., 2000) as measured during the same analytical session.

The Pb isotopic compositions were determined at the Geological Survey of Japan/AIST. Average isotope ratio data from both laboratories was found to be within ~1 s.d., and were within similar levels of uncertainty of the poly-spike SRM 981 values of Taylor et al. (2015). Consequently data presented are not internally adjusted or normalized. Pb separation was achieved using AG1-X8 200–400 mesh anion exchange resin. Procedural Pb blanks were <30 pg, and considered negligible relative to the amount of sample analyzed. Pb isotopic measurements were made in multi-dynamic collection mode using the double spike technique (Southampton-Brest-Lead 207-204 spike SBL74:Ishizuka et al., 2003; Taylor et al., 2015). Natural (unspiked) measurements were made on

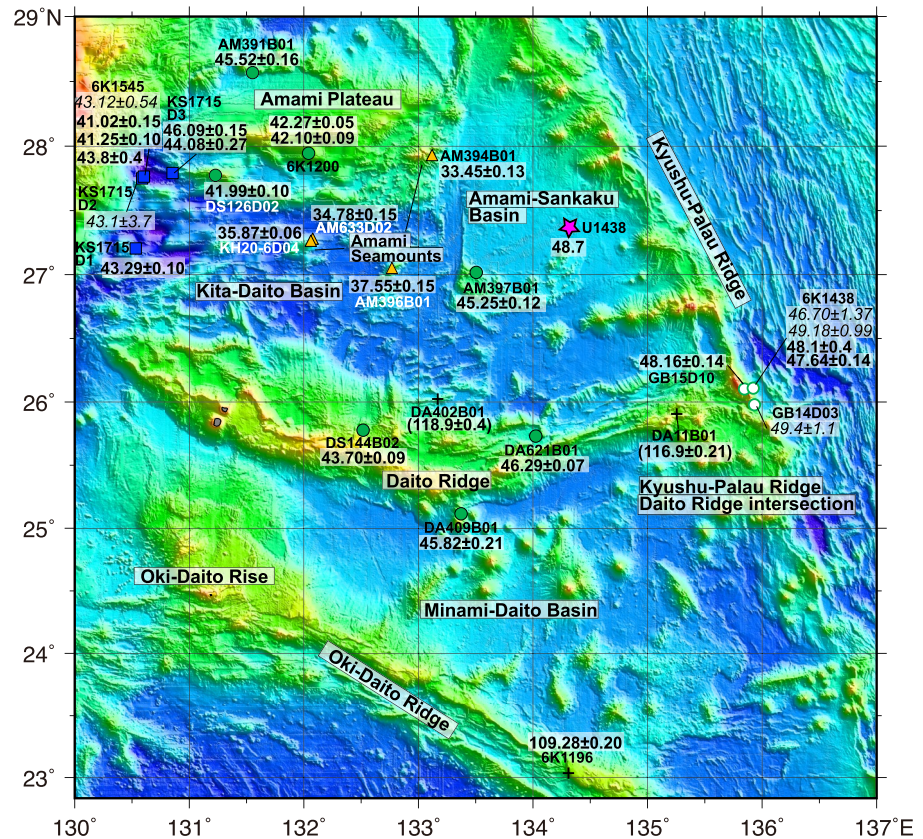


Figure 2. Distribution of $^{40}\text{Ar}/^{39}\text{Ar}$ and zircon U-Pb ages (in Ma) obtained for igneous rocks for the studied samples. U-Pb ages are shown in italics. Ages in parentheses are from Ishizuka, Taylor, et al. (2011).

60%–70% of collected Pb, giving ^{208}Pb beam intensities of $2.5\text{--}3 \times 10^{-11}\text{A}$. Fractionation-corrected Pb isotopic compositions and internal errors were obtained by a closed-form linear double-spike deconvolution (Johnson & Beard, 1999). The reproducibility of Pb isotopic measurements (external error: 2 s.d.) by double spike is <200 ppm for all $^{208}\text{Pb}/^{204}\text{Pb}$ ratios. Measured values for NBS SRM-981 during the measurement period were $^{206}\text{Pb}/^{204}\text{Pb} = 16.9407 \pm 0.0039$, $^{207}\text{Pb}/^{204}\text{Pb} = 15.5010 \pm 0.0050$, and $^{208}\text{Pb}/^{204}\text{Pb} = 36.724 \pm 0.012$ (2 s.d., $n = 21$).

5. Results

5.1. $^{40}\text{Ar}/^{39}\text{Ar}$ and U-Pb Ages

20 samples have been dated by the laser-heating $^{40}\text{Ar}/^{39}\text{Ar}$ dating technique (Figure 2, Table 1: Age spectra and raw data are presented as Figure S1 and Table S2 in Supporting Information S1), and 5 samples have been dated by zircon U-Pb dating (Figures 2 and 3: Data table and representative cathodoluminescence images with analyzed points are included as Figure S2 and Table S3 in Supporting Information S1).

Andesitic rocks from the basin floor of the Kita-Daito Basin show age range between 41.04 and 46.11 Ma (Table 1). KS1715D01R03 provided poorly defined inverse isochron, because all the plateau-forming steps show low atmospheric contamination and very small dispersion in $^{36}\text{Ar}/^{40}\text{Ar}$ (and $^{39}\text{Ar}/^{40}\text{Ar}$). Even though initial Ar isotopic ratio cannot be determined precisely, we interpret that the highly radiogenic character of the plateau-forming steps imply that they are free from disturbance by alteration, and it is unlikely that the sample carries extraneous ^{40}Ar based on the mineralogy of the groundmass of the sample (highly crystalline and mostly composed of plagioclase with minor amount of pyroxene). The weighted average of ages from the plateau can be regarded as a reasonable estimate for the eruption age of this sample.

Table 1
Results of $^{40}\text{Ar}/^{39}\text{Ar}$ Stepwise-Heating Analyses

Irradiation No.	Analysis No.	Sample No.	Seamount name	Total age ($\pm 1\sigma$)			Plateau age ($\pm 1\sigma$)			fraction of ^{39}Ar (%)		
				integrated age (Ma)	inv. isochron age (Ma)	$^{40}\text{Ar}/^{36}\text{Ar}$ intercept	MSWD	weighted average (Ma)	inv. isochron age (Ma)		$^{40}\text{Ar}/^{36}\text{Ar}$ intercept	MSWD
Northern Philippine Sea Seamounts												
JMTR0403-1	U05005	DS126D02C10	Kakeroma	42.00 \pm 0.10	41.98 \pm 0.22	335 \pm 15	0.81	41.99 \pm 0.10	42.00 \pm 0.22	297 \pm 38	0.53	99.3
JRR40404-1	U05058	AM391B01C01	Onotsu	45.80 \pm 0.10	45.4 \pm 0.3	356 \pm 22	3.29	45.52 \pm 0.16	43.9 \pm 0.6	448 \pm 54	0.84	58.3
JRR40404-1	U05064	AM397B01C01	Inokawa	46.27 \pm 0.08	45.5 \pm 0.3	385 \pm 18	2.52	45.25 \pm 0.12	44.7 \pm 0.5	751 \pm 339	0.65	50.1
JRR40504-1	U06059	DA409B01C02		45.4 \pm 0.4	43.5 \pm 1.7	960 \pm 454	11.23	45.82 \pm 0.21	45.4 \pm 0.9	951 \pm 853	2.61	64.8
JRR30902-2	U10200	DA621B01C02		46.68 \pm 0.04	46.4 \pm 0.3	378 \pm 27	3.50	46.29 \pm 0.07	45.5 \pm 0.4	2,521 \pm 1,304	0.84	57.0
JMTR0502-1	U06064	DS144B02 120-130		43.92 \pm 0.05	43.32 \pm 0.24	415 \pm 24	11.42	43.70 \pm 0.09	43.3 \pm 0.4	764 \pm 565	3.00	55.0
JRR31003-1	U11314	6K1200R13		41.02 \pm 0.09	47.5 \pm 1.4	-1,581 \pm 1,315	4.32	42.10 \pm 0.09	41.3 \pm 0.4	737 \pm 198	1.14	56.9
KUR2001	U21012	6K1200R13		41.067 \pm 0.022	41.2 \pm 0.3	338 \pm 55	10.35	42.27 \pm 0.05	41.96 \pm 0.24	438 \pm 59	3.28	50.8
Kita-Daito Basin												
KUR1703	U18100	KS1715D01R03	Isen	43.03 \pm 0.07	43.23 \pm 0.24	230 \pm 10	1.89	43.29 \pm 0.10	44.3 \pm 0.3	-122 \pm 30	0.94	69.1
KUR1703	U18249	KS1715D03R01		44.0 \pm 0.3	44.2 \pm 0.5	276 \pm 13	2.39	44.08 \pm 0.27	44.5 \pm 0.4	274 \pm 10	1.49	95.1
KUR1803	U19229	KS1715D03R02		45.26 \pm 0.11	44.1 \pm 0.7	749 \pm 197	10.50	46.09 \pm 0.15	46.1 \pm 0.3	294 \pm 42	2.75	65.2
KUR1904	U20001	6K1545R06	Yoro	45.0 \pm 0.3	46.4 \pm 0.5	285 \pm 3	2.18	43.8 \pm 0.4	44.4 \pm 0.6	292 \pm 3	1.29	56.9
OSU06-02	U20334	6K1545R04	Yoro	42.04 \pm 0.09	42.4 \pm 0.5	289 \pm 6	7.79	41.25 \pm 0.10	41.7 \pm 0.6	290 \pm 6	2.20	54.2
KUR2001	U21019	6K1545R09	Yoro	40.82 \pm 0.13	44.4 \pm 0.8	267 \pm 6	2.87	41.02 \pm 0.15	43.5 \pm 1.2	276 \pm 10	0.98	60.6
Kyushu-Palau Ridge - Daito Ridge intersection												
OSU01-01	U17109	6K1438R11 biotite	Minami-Koho	48.0 \pm 0.4	48.4 \pm 0.4	208 \pm 42	0.55	48.1 \pm 0.4	48.4 \pm 0.4	208 \pm 42	0.55	100.0
KUR2001	U21018	6K1438R11 biotite	Minami-Koho	47.54 \pm 0.14	47.5 \pm 0.3	310 \pm 24	1.01	47.64 \pm 0.14	47.5 \pm 0.3	310 \pm 24	1.01	100.0
OSU02-02	U17325	GB15D10R01 biotite	Minami-Koho	48.02 \pm 0.014	48.3 \pm 0.3	261 \pm 45	1.44	48.16 \pm 0.14	48.2 \pm 0.3	280 \pm 36	0.95	99.3
Amami Seamounts												
JRR40404-1	U05059	AM396B01C01	Kanami	37.45 \pm 0.11	36.7 \pm 0.6	390 \pm 31	19.3	37.55 \pm 0.15	37.0 \pm 0.4	468 \pm 82	1.32	72.3
JRR40404-1	U05065	AM394B01C02	Yuwana	33.57 \pm 0.16	31.9 \pm 1.1	537 \pm 103	113.1	33.45 \pm 0.13	33.33 \pm 0.29	893 \pm 478	1.50	54.5
JRR31004-1	U11362	AM633D02C01	Tete	33.31 \pm 0.12	26.0 \pm 2.3	4,267 \pm 3,150	0.70	34.78 \pm 0.15	33.9 \pm 0.7	813 \pm 305	0.16	59.3
KUR2010	U21039	KH20-6D04R01g	Tete	35.94 \pm 0.05	35.78 \pm 0.19	311 \pm 6	2.49	35.87 \pm 0.06	35.85 \pm 0.20	305 \pm 10	2.36	85.8
Mesozoic Daito Ridge Group												
KUR2001	U21015	6K1196R09		107.86 \pm 0.13	107.3 \pm 0.8	363 \pm 32	13.89	109.28 \pm 0.20	109.0 \pm 0.6	323 \pm 14	2.39	61.1

Note. inv. isochron age: Inverse isochron age. MSWD: Mean square of weighted deviates ((SUMS/(n-2))^{0.5}) in York (1969). Integrated ages were calculated using sum of the total gas released. $\lambda_0 = 4.962 \times 10^{-10} \text{y}^{-1}$, $\lambda_e = 0.581 \times 10^{-10} \text{y}^{-1}$, $^{40}\text{K}/\text{K} = 0.01167\%$ (Steiger & Jäger, 1977). Atmospheric $^{40}\text{Ar}/^{36}\text{Ar}$: 295.5.

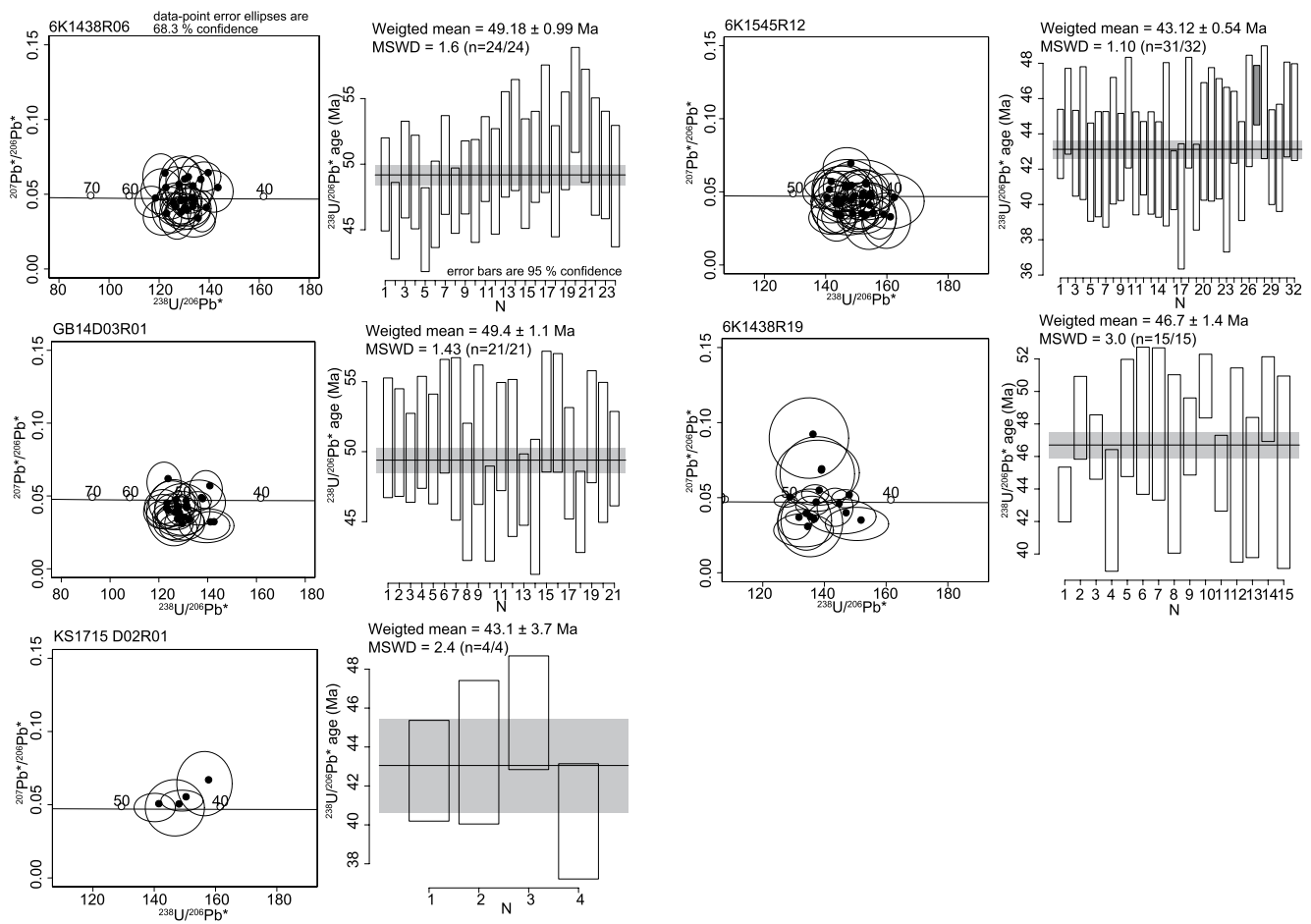


Figure 3. Tera-Wasserburg concordia diagrams and weighted mean ages from zircon U-Pb dating.

Zircon U-Pb dating of coarse-grained andesitic rocks (6K1545R12 and KS1715D02R01) from the Kita-Daito Basin at 5400–5800 mbsl (m below sea level) gave ages of 43.12 ± 0.54 Ma and 43.05 ± 3.70 Ma, respectively (Figures 2 and 3).

Andesites and basalts from the Northern Philippine Sea Seamounts gave age range between 42.10 and 46.29 Ma (Figure 2). DA610B01C01, AM391B01C01, and AM397B01C01 show weak staircase pattern with decreasing age with increasing laser power (i.e., higher outgas temperature) and AM390B04C01 shows hump at middle temperature steps, implying redistribution of Ar in the sample due to recoil effect at irradiation. But highly radiogenic composition of these steps along with differentiated composition of the samples (unlikely presence of host for mantle-derived ^{40}Ar) led us to interpret that the ages obtained from these steps with consistent ages are likely to be good estimate for the eruption ages for these samples.

Basalts from the Amami Seamounts gave ages between 33.50 and 37.55 Ma, which are significantly younger than the ages of the rocks from the basin floor (Figure 2).

Dioritic samples from the KPR–Daito Ridge intersection were dated on biotite separates by stepwise heating analysis. For the sample 6K1438R11, duplicate analyses gave consistent plateau ages of 48.1 ± 0.4 Ma and 47.66 ± 0.14 Ma (Figure 2). Small dispersion of the data for 6K1438R11 with highly radiogenic isotopic composition on isotopic ratio plot made the precise determination of initial $^{40}\text{Ar}/^{36}\text{Ar}$ difficult. Another sample from the KPR–Daito Ridge intersection (GB15D10R01) returned an indistinguishable plateau age of 48.16 ± 0.14 Ma (Figure 2).

Zircon U-Pb dating of a hornblende diorite sample (6K1438R06) from 3723 mbsl gave an age of 49.18 ± 0.99 Ma, while a biotite tonalite sample (6K1438R19) from 2480 mbsl gave an age of 46.7 ± 1.4 Ma (Figures 2 and 3). An

andesite porphyry (GB14D03R01) from the southernmost part of the KPR–Daito Ridge intersection also gave a similar age of 49.4 ± 1.1 Ma (Figures 2 and 3).

Porphyritic andesite from the southeastern part of the Oki-Daito Ridge (6K1196R09) returned slightly disturbed age spectrum with increasing ages with increasing laser output (i.e., temperature). 13 steps at higher temperature steps give indistinguishable ages with a weighted average of 109.30 ± 0.20 Ma (Figure 2). Inverse isochron age of 109.0 ± 0.6 Ma is consistent with the weight average age and an $^{36}\text{Ar}/^{40}\text{Ar}$ intercept is identical with atmospheric ratio within 2σ uncertainty. The weighted average age is regarded as the reasonable estimate of crystallization age of this andesite.

5.2. Whole Rock Chemical Compositions

Volcanic rocks from the Northern Philippine Sea Seamounts are mainly andesite with minor amount of basalts, and categorized as medium to high K with rare shoshonitic compositions. These rocks have significantly higher K content than most of the volcanic rocks from the KPR and modern Izu-Bonin arc front (Figure 4a; Table S4 in Supporting Information S1).

These basalts/andesites also have higher Al_2O_3 , significantly higher K_2O and comparable MgO and TiO_2 contents to the contemporaneous Eocene Hahajima Group rocks from the Izu-Bonin forearc (Ishizuka et al., 2020; Kanayama et al., 2014), which are taken to represent the post-45 Ma calcalkaline to tholeiitic arc magmatism that followed the boninite magmatism (Figures 4a–4d). They have significantly higher TiO_2 and lower MgO relative to Eocene boninites from the Izu-Bonin forearc (Figures 4c and 4d). In addition, they are also distinct from Eocene MORB-like basalts from the Amami Sankaku Basin by having significantly higher K_2O (Figure 4a).

These characteristics are shared with Eocene andesitic rocks from the basin floor of the Kita-Daito Basin, and those from the KPR–Daito Ridge intersection (Figure 4). This means that this type of volcanism was distributed from the westernmost of the Kita-Daito Basin ($130^\circ30'\text{E}$) to KPR–Daito Ridge intersection (136°E); an E-W distance of over 550 km. It also covered the area between the Amami Plateau in the north ($28^\circ30'\text{N}$) and Daito Ridge to the south (25°N); a N-S distance of around 450 km. Gabbroic and granitic rocks from the KPR–Daito Ridge intersection also have a compositional range or trend with higher K_2O than the Eocene Hahajima Group, the KPR, and the Quaternary Izu-Bonin frontal arc (Figure 4a).

MORB-normalized trace element pattern shows that the volcanic rocks from the Northern Philippine Sea Seamounts and Kita-Daito Basin have an enrichment in LILE (large-ion lithophile elements) and a depletion in Nb, Ta, Zr, Hf (Figure 5). These characteristics are reflected in the elevated Ba/Ta and Th/Ta relative to MORB, and OIB (Figure 6), implying a contribution of hydrous fluid or melt from the subducting slab (e.g., Pearce et al., 2005). Th/Yb for these rocks is significantly higher than the Eocene forearc volcanic rocks at a given Ta/Yb, while Ba/Yb is comparable or slightly higher than Eocene boninites, but clearly higher than contemporaneous Hahajima Group (Figure 6).

The Northern Philippine Sea Seamounts have high Sr, Sr/Y, La/Sm and Dy/Yb relative to the contemporaneous Eocene Izu-Bonin arc (Figure 7), and these characteristics are shared with those from the Kita-Daito Basin. Dy/Yb generally decreases with increasing SiO_2 , but samples from the central part of the Amami Plateau (Dive 6K1200) are the exception with significantly higher (Dy/Yb). The 6K1200 samples have high Sr (1200–1500 ppm) accompanied by lower Y (13–17 ppm) compared to other Northern Philippine Sea Seamounts rocks. Sr/Y and Dy/Yb are positively correlated (Figure 7e). On the other hand, La/Yb for the Northern Philippine Sea Seamounts is significantly higher than Eocene Izu-Bonin rocks, but comparable to KPR, and shows overall positive correlation with SiO_2 , again with much higher ratios for the samples from 6K1200 dive (Figure 7d).

The whole rock geochemical characteristics of the Northern Philippine Sea Seamounts and the Kita-Daito Basin volcanics are shared with the KPR–Daito Ridge intersection and Mesozoic igneous rocks exposed on the Daito Ridge Group (Daito Ridge and Oki-Daito Ridge: Figure 7), that is, they show relatively higher Sr, Sr/Y, Dy/Yb, La/Sm and La/Yb compared to those from Eocene Izu-Bonin arc, and enriched in Ba and Th relative to MORB and OIB.

Olivine basalts from the Amami Seamounts show distinct geochemical characteristics from other volcanic rocks from the basin (Figures 4–7). These basalts lack significant enrichment in fluid-mobile elements and depletion

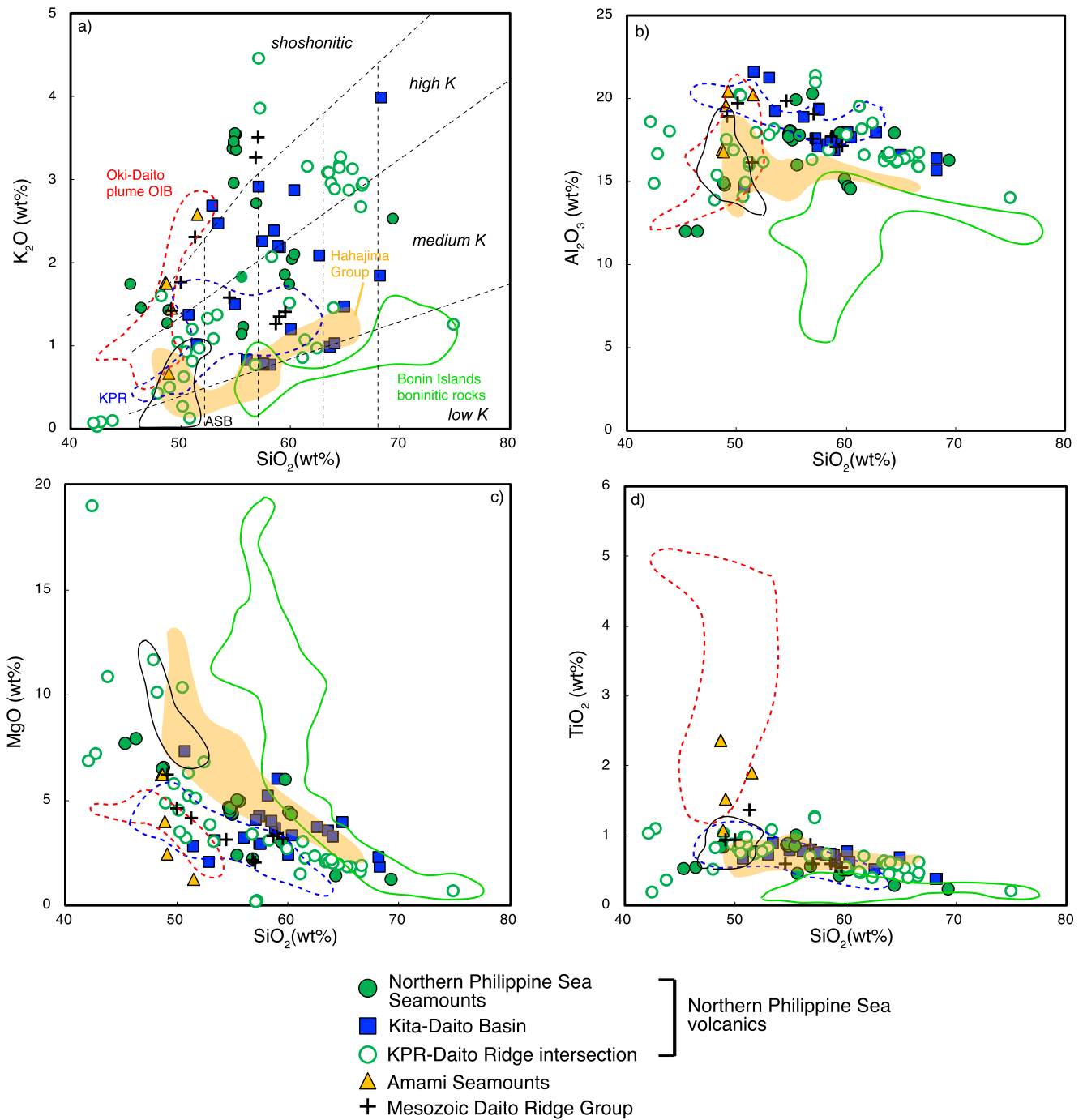


Figure 4. Major element composition of volcanic rocks from the studied area. Variation of SiO_2 with (a) K_2O , (b) Al_2O_3 , (c) MgO , (d) TiO_2 . Data source: Boninitic rocks from the Bonin Ridge and Hahajima Group rocks: Kanayama et al. (2012, 2014); Li et al. (2019); Ishizuka et al. (2020). KPR rocks: Ishizuka, Taylor, et al. (2011). Oki-Daito plume OIB: Ishizuka et al. (2013). Basalts from the Amami Sankaku Basin (ASB): Ishizuka et al. (2018). Rock subdivision in Figure 4a is adopted from Le Maitre (1989) and Rickwood (1989).

in HFSE relative to other incompatible elements, but generally show higher incompatible element content than N-MORB.

Based on similarity in age, geochemistry and geographical location, we collectively call the volcanics from the Northern Philippine Sea Seamounts, Kita-Daito Basin and KPR–Daito Ridge intersection “Northern Philippine Sea volcanics.”

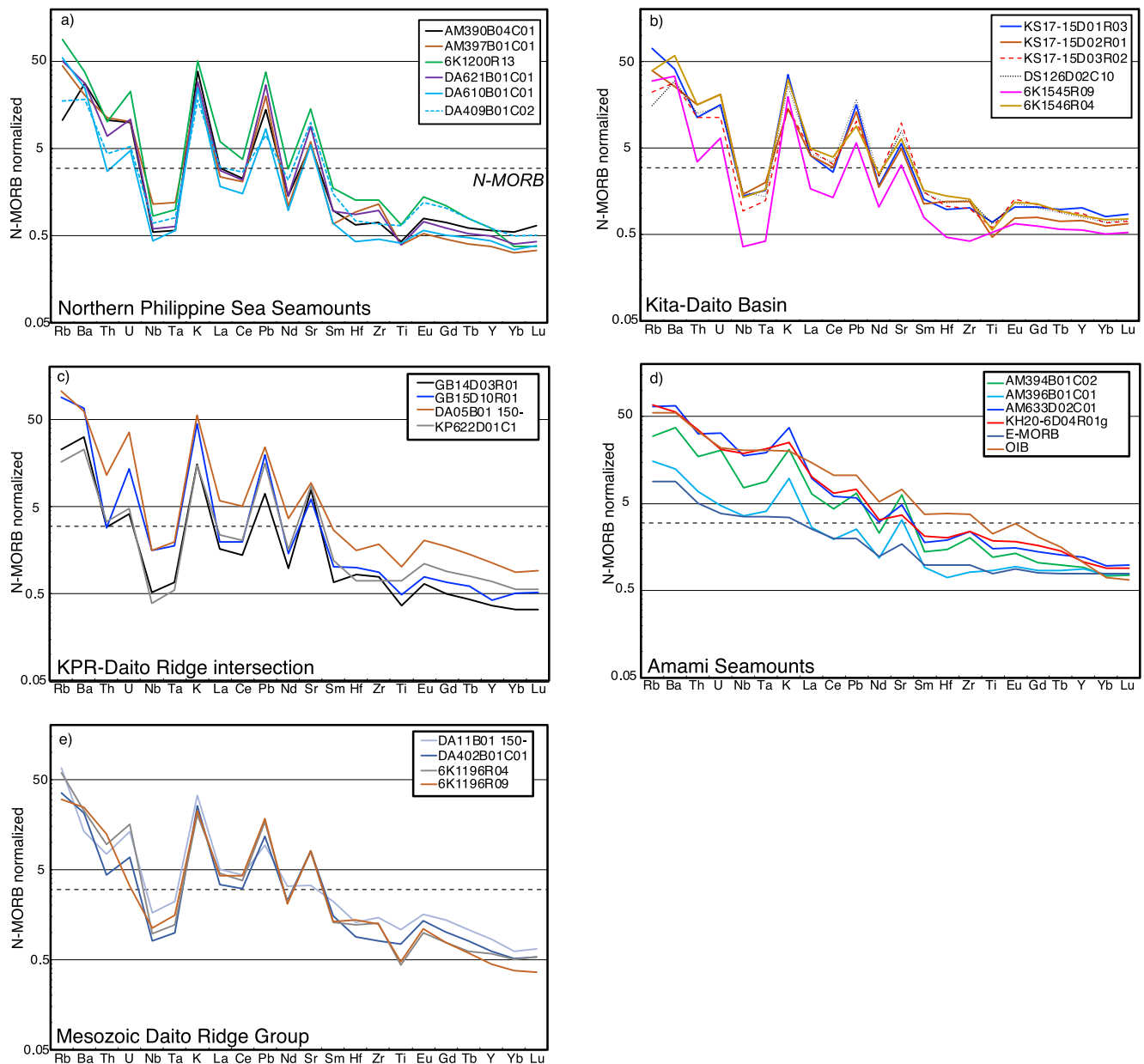


Figure 5. Selected MORB-normalized whole rock compositions of (a) Northern Philippine Sea Seamounts, (b) Kita-Daito Basin, (c) samples from the KPR–Daito Ridge intersection, (d) basalts from the Amami Seamounts, (e) Mesozoic Daito Ridge Group. Normalized to N-MORB of Sun and McDonough (1989).

5.3. Radiogenic Isotopes

5.3.1. Northern Philippine Sea Volcanics

Pb isotope ratios of the Northern Philippine Sea volcanics lie on or very close to NHRL (Hart, 1984) and hence are distinct from most of the Philippine Sea ocean crust (Philippine Sea MORB) and Izu-Bonin arc rocks (Figures 8a–8c). They also have higher $^{206}\text{Pb}/^{204}\text{Pb}$ than the Philippine Sea MORB (>18.5 compared to <18.1). These characteristics are somewhat similar to the Eocene Hahajima Group rocks in the Izu-Bonin forearc of the same age range. The Northern Philippine Sea volcanics show variable $\Delta^{207}\text{Pb}/^{204}\text{Pb}$ and $\Delta^{208}\text{Pb}/^{204}\text{Pb}$ with almost constant $^{206}\text{Pb}/^{204}\text{Pb}$, which sharply contrasts with boninites from the Bonin Islands which have steeply increasing $\Delta^{207}\text{Pb}/^{204}\text{Pb}$ and $\Delta^{208}\text{Pb}/^{204}\text{Pb}$ with increasing $^{206}\text{Pb}/^{204}\text{Pb}$. The Northern Philippine Sea volcanics do share Pb isotopic characteristics with boninites from outboard of the Bonin Islands drilled at IODP Exp. 352 (Li et al., 2019) by having $\Delta^{207}\text{Pb}/^{204}\text{Pb}$ and $\Delta^{208}\text{Pb}/^{204}\text{Pb}$ of around 0 (Figures 8b and 8c). Despite their wide

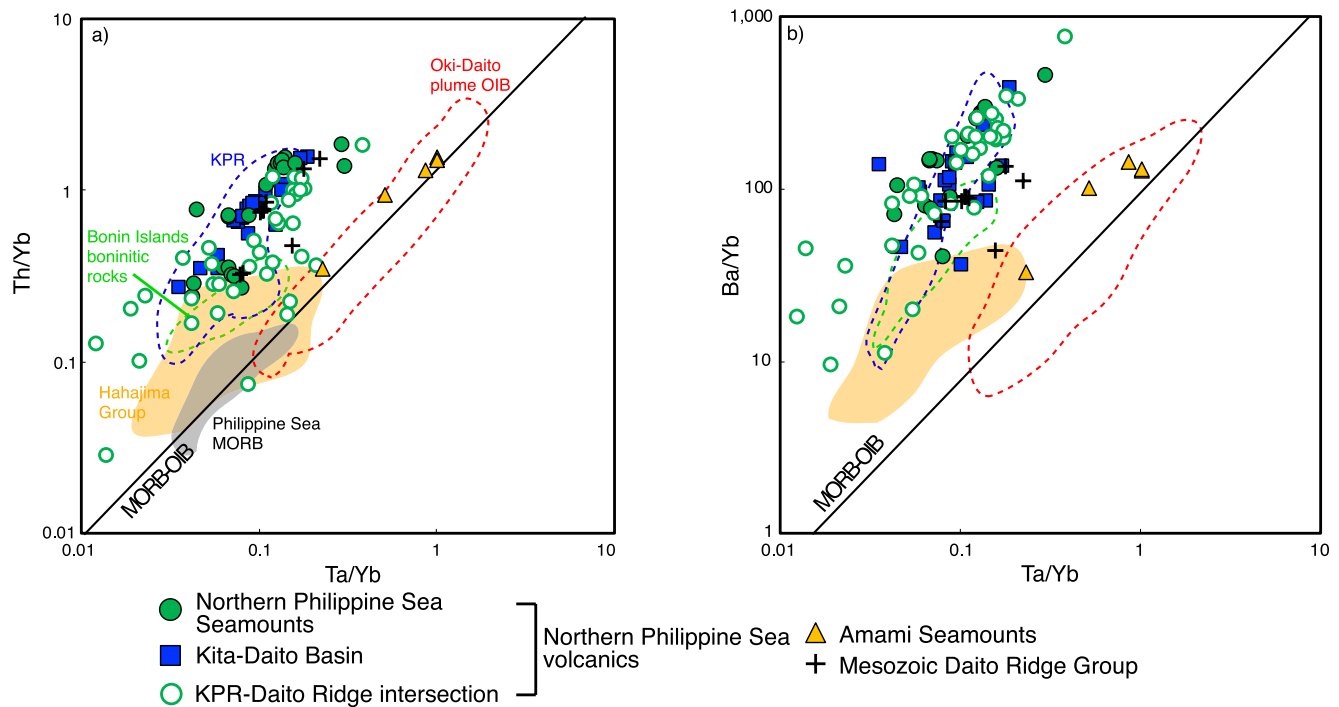


Figure 6. (a) Th/Yb-Ta/Yb and (b) Ba/Yb-Ta/Yb plots to identify Th and Ba enrichment in the studied rocks relative to mantle-derived melts (MORB and OIB). Line representing the array of global MORB-OIB composition is from Pearce et al. (2005). Philippine Sea MORB composition: Hickey-Vargas (1991, 1998), Hickey-Vargas et al. (2018), Ishizuka et al. (2009, 2010, 2013), Savov et al. (2006). Other data sources are as Figure 4.

distribution, the Northern Philippine Sea volcanics have a relatively small compositional range relative to the other volcanic groups.

Pb-Nd isotopic co-variation highlights some differences between the Eocene Izu-Bonin arc rocks and the Northern Philippine Sea volcanics (Figure 8d). For example, the Northern Philippine Sea volcanics show negative correlation between $^{206}\text{Pb}/^{204}\text{Pb}$ and $^{143}\text{Nd}/^{144}\text{Nd}$, with significantly higher $^{143}\text{Nd}/^{144}\text{Nd}$ than Eocene Bonin Island boninites, but only slightly lower than Eocene Hahajima Group (Figure 8d). The Northern Philippine Sea volcanics again have similar Pb-Nd isotope systematics to some axial boninites from the IODP Exp. 352 (Figure 8d).

Sr isotopes of the Northern Philippine Sea volcanics are also clearly distinct from Eocene Izu-Bonin volcanics, with showing significantly lower $^{87}\text{Sr}/^{86}\text{Sr}$ than boninites and slightly lower than Hahajima Group.

The Northern Philippine Sea volcanics are enriched in fluid-mobile elements such as Ba and Pb, and have higher Sr and Pb isotope ratios and fluid-mobile element/LREE ratios relative to lavas from a Philippine Sea MORB-type source (Figures 9a and 9b). These trace element ratios vary with relatively minor changes in Sr and Pb isotope ratios, which results in near vertical trends on these isotope versus trace element ratio plots (Figures 9a and 9b).

The Northern Philippine Sea volcanics are distinct from Eocene boninites in terms of Nd isotopes versus LREE enrichment or Th/La (Figures 9c and 9d), specifically they trend to much higher La/Yb, and Th/La and lower $^{143}\text{Nd}/^{144}\text{Nd}$ than the boninites. The Northern Philippine Sea volcanics overlap with Eocene Hahajima Group at their lowest Th/La, but they do not overlap in La/Yb against $^{143}\text{Nd}/^{144}\text{Nd}$.

Hf/Nd - $^{143}\text{Nd}/^{144}\text{Nd}$ relationship clearly distinguish the Northern Philippine Sea volcanics from other Eocene Izu-Bonin arc rocks and MORB-type basalts from the Philippine Sea (Figure 9e). The Northern Philippine Sea volcanics have lower Hf/Nd than other Eocene arc rocks, and comparable $^{143}\text{Nd}/^{144}\text{Nd}$ to the material derived from altered Pacific ocean crust (Li et al., 2019).

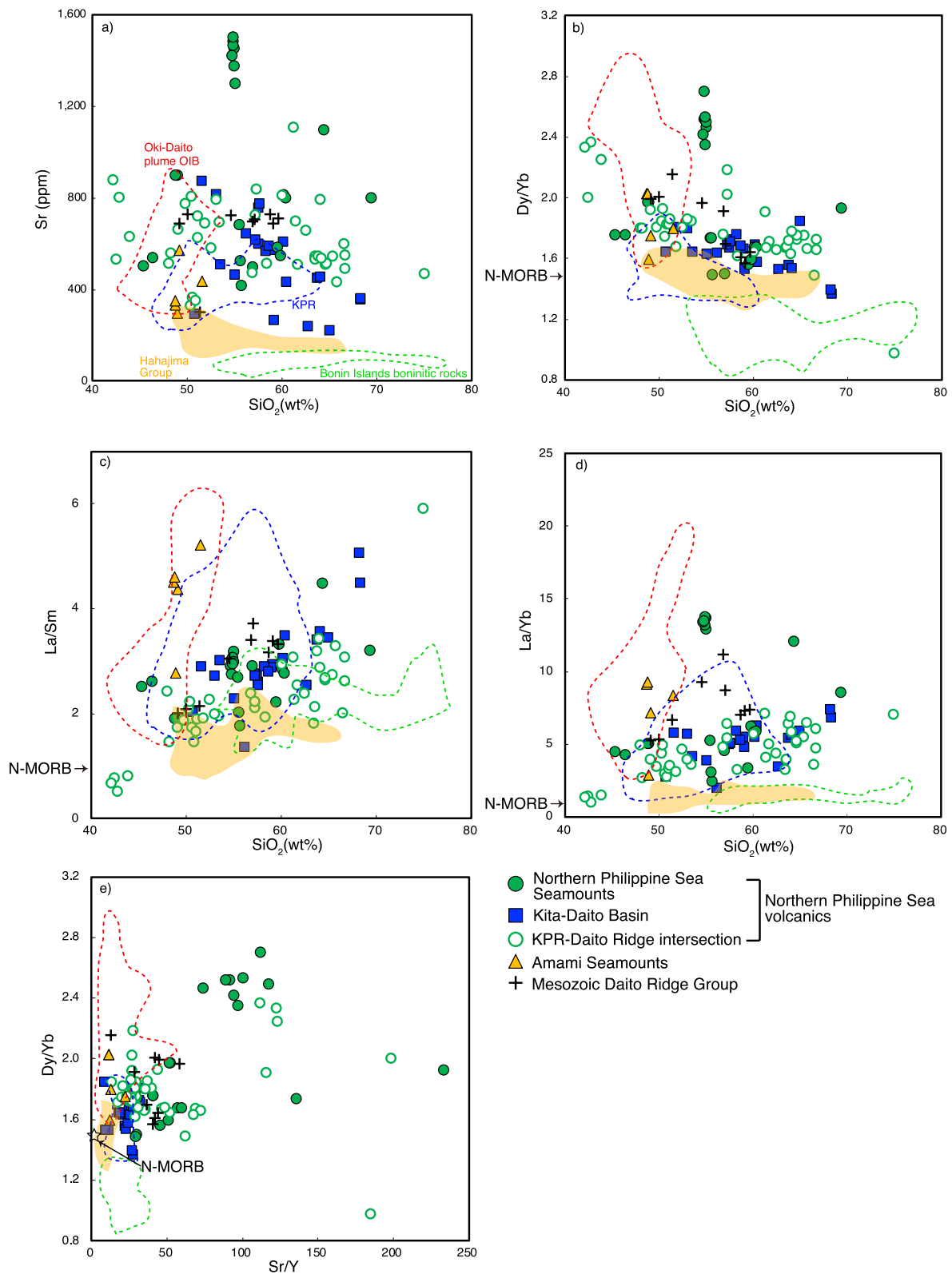


Figure 7. Incompatible trace element concentration and ratios for the studied igneous rocks. Variation of (a) Sr content, (b) Dy/Yb, (c) La/Sm, (d) La/Yb with SiO_2 wt%, and (e) Dy/Yb with Sr/Y. Data sources are the same as Figure 4.

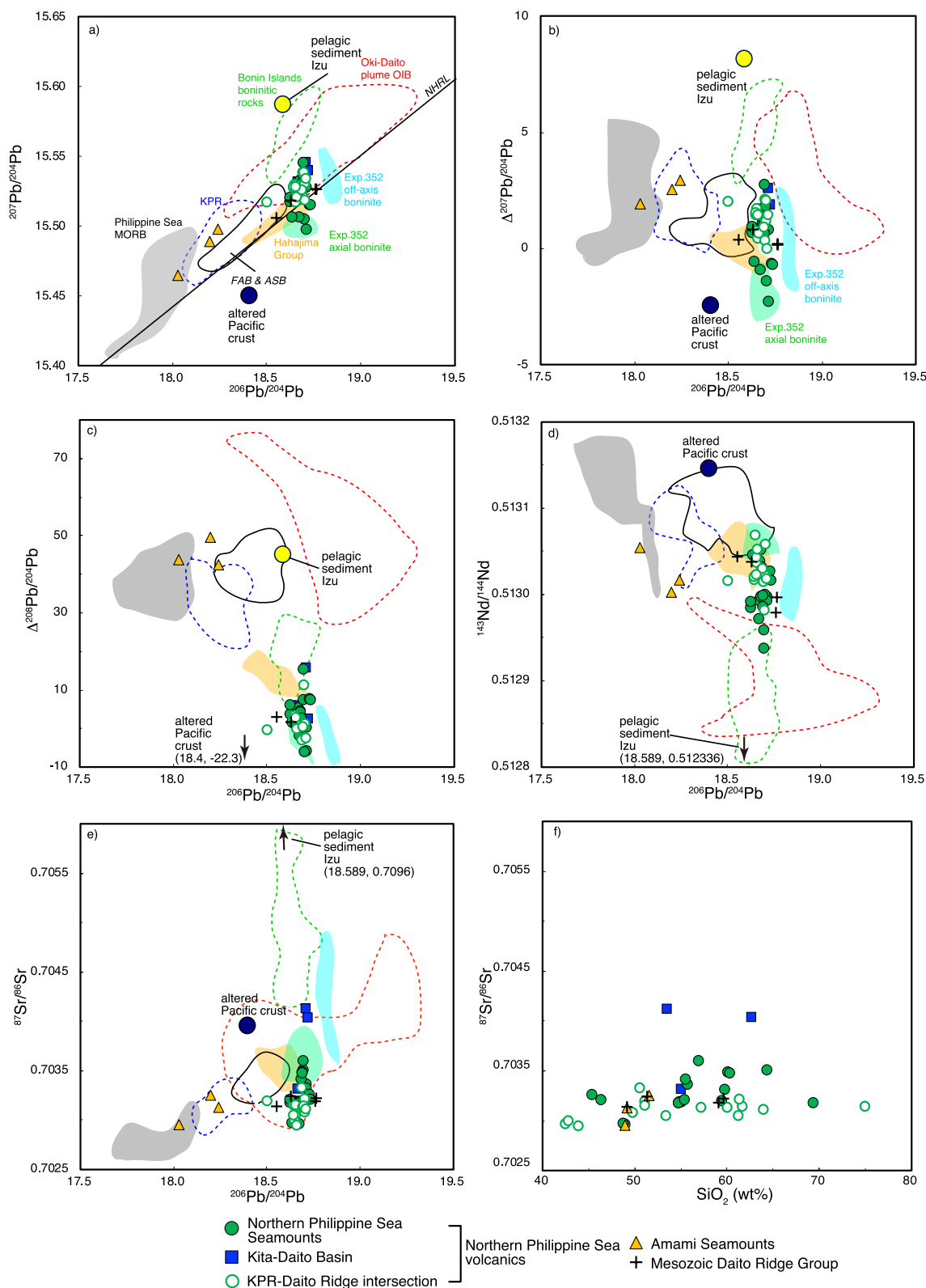


Figure 8.

5.3.2. Amami Seamounts

Basalts from the Amami Seamounts have relatively low $^{206}\text{Pb}/^{204}\text{Pb}$, but distinctly higher $\Delta^{207}\text{Pb}/^{204}\text{Pb}$ and $\Delta^{208}\text{Pb}/^{204}\text{Pb}$ than other volcanics in the basin (Figures 8b and 8c). These characteristics are similar to basalts from the extinct spreading center of the Shikoku Basin: the Kinan Seamount Chain (Figure 1a) reported by Ishizuka et al. (2009).

5.3.3. Daito Ridge Group

Volcanic rocks from the Daito Ridge Group have similar Pb isotope ratios and trends to the Northern Philippine Sea volcanics in having $\Delta^{207}\text{Pb}/^{204}\text{Pb}$ and $\Delta^{208}\text{Pb}/^{204}\text{Pb}$ of ~ 0 , with $^{206}\text{Pb}/^{204}\text{Pb}$ of around 18.5–18.7 (Figures 8a–8c). These volcanic rocks also have similar Pb–Nd and Sr–Nd covariations and have overlapping LREE/HREE or Th/La– $^{143}\text{Nd}/^{144}\text{Nd}$ trends to the Northern Philippine Sea volcanics (Figures 9c and 9d).

5.4. Spatial Variation of Geochemistry

The Northern Philippine Sea volcanics and KPR–Daito Ridge intersection volcanics are distributed across a wide area of c. 400×520 km in and around the Daito Ridge group region. Here we examine the potential for a systematic spatial variation in the volcanic geochemistry of the area.

In a north–south direction, there is a slight decrease in $^{143}\text{Nd}/^{144}\text{Nd}$ and an increase in $\Delta^{208}\text{Pb}/^{204}\text{Pb}$ toward the north, although no other systematic variation can be observed in trace element and isotopic ratios (Figures 10a–10g). In east–west direction, that is, perpendicular to the KPR, no systematic variation in isotopic composition can be recognized (Figures 10h–10k). These plots also show that isotopic compositions of the KPR volcanics near the KPR–Daito Ridge intersection are clearly distinct from those from the KPR–Daito Ridge intersection. Trace element ratios which are not affected by crystal fractionation, especially those related to slab-derived material, are also examined (Fig. 10l–10n). Th/La and Ba/La, for example, do not show a systematic E–W variation, even though samples from the westernmost part of the Kita–Daito Basin show larger range extending toward higher ratios. Nb/Zr ratio are generally similar across the studied area.

6. Discussion

6.1. Origin of “Arc” Geochemical Signature in the Northern Philippine Sea

The Northern Philippine Sea volcanics show clear enrichment in LILE and depletion in Nb, Ta, Zr and Hf, which are the typical characteristics of arcs. However, the apparent limited duration of Northern Philippine Sea volcanism, as well as lack of geochemical evidence for arc polarity, implies that this magmatism, and its arc signature, was caused by a mechanism other than contemporaneous or on-going subduction. Potentially, such a mechanism could be the rifting and extension to form the Kita–Daito Basin (Figure 11). Examples have been reported from the modern Izu–Bonin–Mariana arc, for example, Sumisu Rift area and northern tip of Mariana Trough (e.g., Hochstaedter et al., 1990; Ishizuka et al., 2002, 2010), and Ryukyu arc (Okinawa Trough: Shinjo et al., 1999). Such magmatism in the early stages of intra-oceanic arc rifting is characterized by a slab-derived signature (Hochstaedter et al., 1990; Ishizuka et al., 2010; Pearce et al., 2005), but this is subdued relative to the volcanic front (e.g., Hochstaedter et al., 1990). Potentially, this rifting-associated magmatism with a slab-signature could be a product of decompression melting of lithospheric mantle that had been metasomatized by an earlier subduction system. This magmatism is eventually replaced by basalt magmatism caused by upwelling asthenospheric mantle, as is thought to be the case for the Mariana Trough (e.g., Pearce et al., 2005). The basalt magma produced at this stage is without or with only a minor slab-derived contribution.

Terranes belonging to the Daito Ridge Group are known to be Mesozoic remnant arcs, which is reinforced by the ages of crust determined in this study (Figure 11), and their slab-derived geochemical signature (Figure 5e).

Figure 8. Radiogenic isotope variation for the studied igneous rocks plotted with potential slab and mantle components (Philippine Sea MORB). (a) $^{207}\text{Pb}/^{204}\text{Pb}$ versus $^{206}\text{Pb}/^{204}\text{Pb}$, (b) $\Delta^{207}\text{Pb}/^{204}\text{Pb}$ versus $^{206}\text{Pb}/^{204}\text{Pb}$, (c) $\Delta^{208}\text{Pb}/^{204}\text{Pb}$ versus $^{206}\text{Pb}/^{204}\text{Pb}$, (d) $^{143}\text{Nd}/^{144}\text{Nd}$ versus $^{206}\text{Pb}/^{204}\text{Pb}$, and (e) $^{87}\text{Sr}/^{86}\text{Sr}$ versus $^{206}\text{Pb}/^{204}\text{Pb}$, and (f) SiO_2 versus $^{87}\text{Sr}/^{86}\text{Sr}$. Assumed composition of subducting igneous crust and sediment are shown (Table S8 in Supporting Information S1). Data for Exp. 352 boninites are from Li et al. (2019). Pelagic sediment outboard of Izu–Bonin arc: Plank et al. (2007), Subducting igneous Pacific crust: Kelley et al. (2003). Philippine Sea MORB: Hickey–Vargas (1991, 1998), Savov et al. (2006), Ishizuka et al. (2009, 2010, 2011b, 2013). Pacific MORB data was compiled from Earthchem data base (<https://www.earthchem.org>). Other data sources as Figure 4.

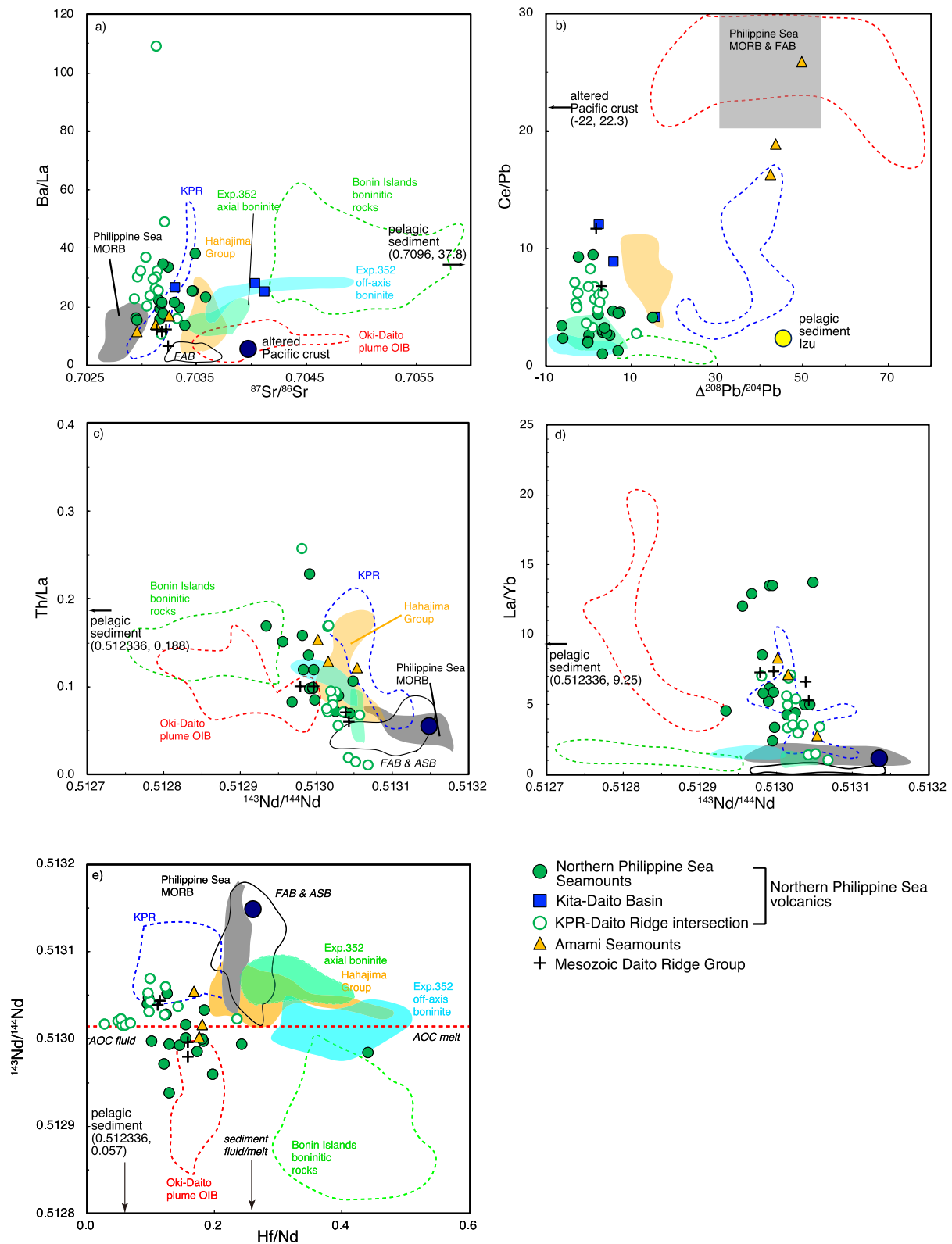


Figure 9. Isotope versus trace element ratio plots for the studied igneous rocks. Data sources as Figure 8. Compositions for AOC (altered ocean crust)-derived fluid and melt and sediment component shown in Figure 9e are from Li et al. (2019).

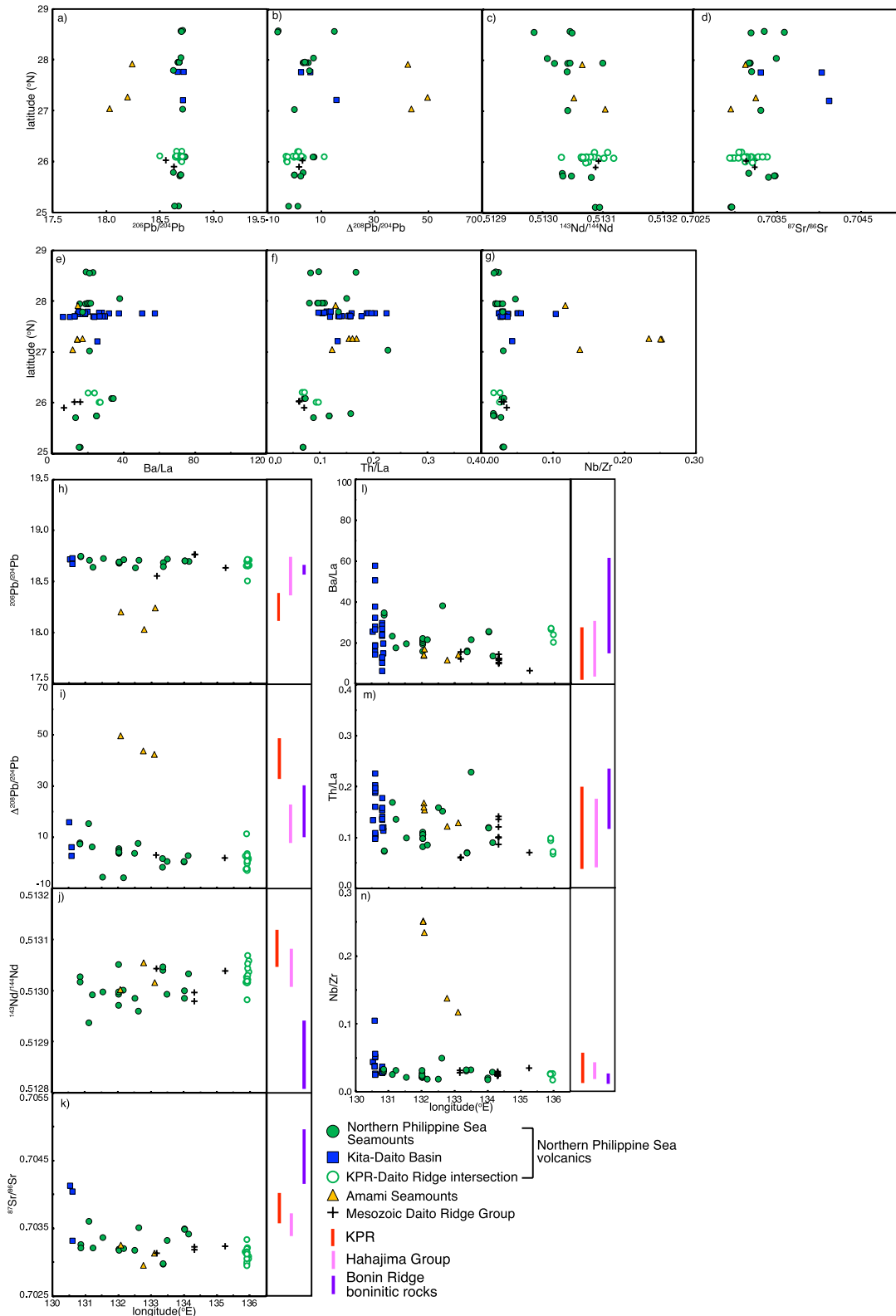


Figure 10. Latitudinal and longitudinal variation of trace element and isotopic ratios of the studied igneous rocks. For the trace element plots, only volcanic rocks are plotted. Compositional range for the KPR, boninitic rocks from the Bonin Ridge and Hahajima Group rocks are shown on the right to the longitudinal plots (Data sources are the same as Figure 4).

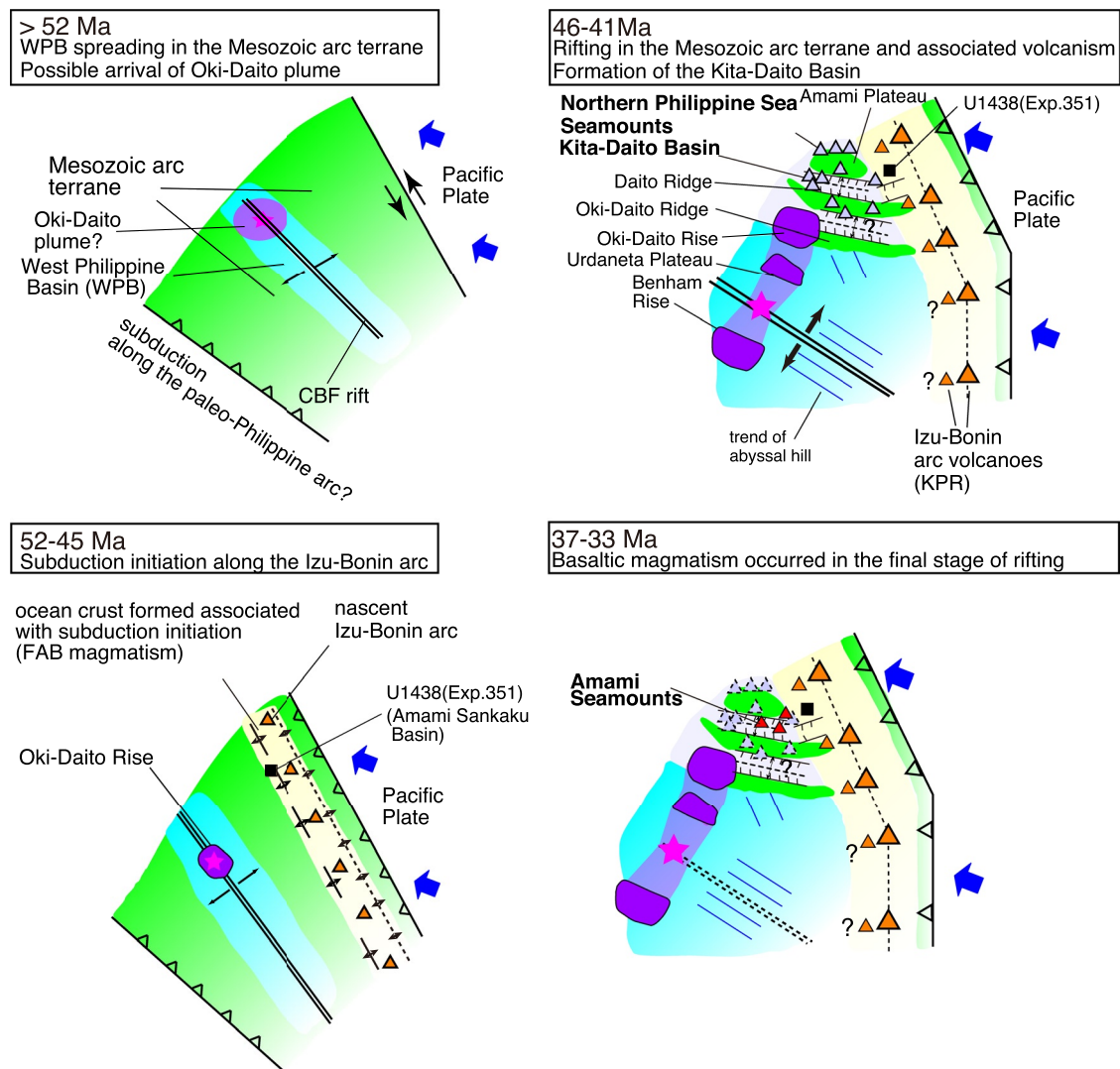


Figure 11. Schematic tectonic history for the northern part of the Philippine Sea Plate including the Kita-Daito Basin and West Philippine Basin. 1) West Philippine Basin had begun spreading before subduction initiation along the Philippine Sea margin. 2) Subduction initiation to form the IBM arc occurred at 52 Ma, while the West Philippine Basin continued to spread. Seafloor spreading took place associated with subduction initiation and formed ocean crust. 3) After 46 Ma, rifting initiated in the Mesozoic terrane, and the Kita-Daito Basin started to develop. Volcanic activity resulting in the Northern Philippine Sea volcanics occurred in the Mesozoic terrane as well as the basin floor of the Kita-Daito Basin. 4) After 37.5 Ma, basaltic magmatism formed volcanic edifices in the Kita-Daito Basin, probably corresponds to the last stage of formation of the Kita-Daito Basin.

Accordingly, it is expected that the mantle beneath the Daito Ridge Group, including the Kita-Daito Basin, was metasomatized by flux from a subducting slab in the Mesozoic, or at least interacted with a Mesozoic arc magma. However, there is no clear evidence of a significant contribution from crustal assimilation (e.g., a correlation between SiO_2 and isotopic compositions: Figure 8f). As such, it is reasonable to assume that the slab-derived signature came from the mantle rather than crust.

The volcanic edifice at 6K1200 dive (Figure 1b) lies in the central part of the Amami Plateau, where relatively thick Mesozoic crust is present (Nishizawa et al., 2014). Nishizawa et al. (2014) showed that the thickness of the crust of the Amami Plateau is around 20 km. However, it is expected to be initially thicker, because (a) rifting is likely to have stretched and thinned the plateau crust, and (b) exposure of granitic rocks on the surface of the plateau indicates significant erosion took place since its formation (Hickey-Vargas, 2005; Shiki et al., 1985). This means that this volcanic edifice is expected to have formed on significantly thicker crust than other edifices. High Sr/Y, La/Yb and Dy/Yb of andesites from 6K1200 dive site appear to be explained by melting with residual garnet or fractional crystallization of garnet, while other Northern Philippine Sea volcanics showing increasing

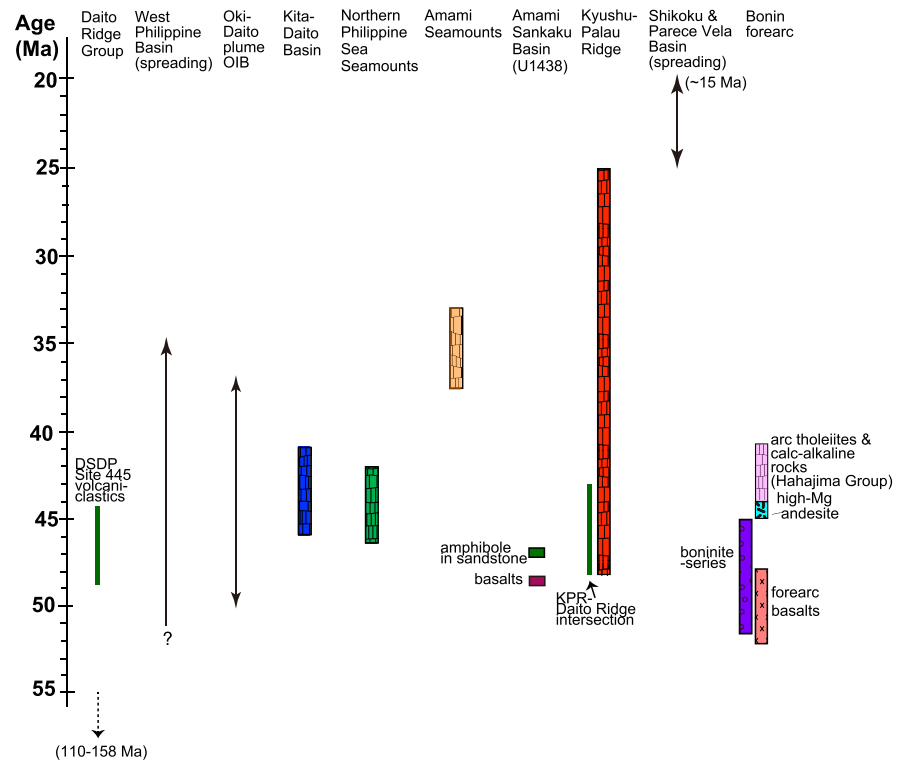


Figure 12. Timeline diagram of magmatism and ocean basin formation in the Philippine Sea. Data sources: Daito Ridge Group: Hickey-Vargas (2005), Ishizuka, Taylor, et al. (2011), Tani et al. (2012), this study, Hickey-Vargas et al. (2013), West Philippine Basin: Deschamps and Lallemand (2002), Sasaki et al. (2014), Oki-Daito plume OIB: Ishizuka et al. (2013), Kita-Daito Basin, Northern Philippine Sea Seamounts, Amami Seamounts: this study, Amami Sankaku Basin: Ishizuka et al. (2018), Waldman et al. (2020), Kyushu-Palau Ridge: Ishizuka, Taylor, et al. (2011), this study, Shikoku and Parece Vela Basin: Ishizuka et al. (2009), Okino (2015), Bonin forearc: Ishizuka, Tani, et al. (2011), Reagan et al. (2019).

La/Yb and decreasing Dy/Yb, which is consistent with fractionation of mainly amphibole but free from garnet (e.g., Macpherson et al., 2006). The andesites from 6K1200 and from the Northern Philippine Sea volcanics share isotopic and other geochemical characteristics, which implies that their sources were similar. This observation suggests that a difference in crystallization assemblage rather than a different mantle sources plays major role in producing the unique geochemical characteristics of 6K1200 andesites.

The Kita-Daito Basin is also potentially underlain by lithospheric mantle metasomatized by Mesozoic subduction. The strong similarity in isotopic composition between the Mesozoic arc volcanics on the Daito Ridge, the Northern Philippine Sea volcanics, and KPR–Daito Ridge intersection volcanics indicates that the same sources were involved in their magma genesis. These characteristics can be explained if the Mesozoic metasomatized mantle was the source of Eocene magmatism in the Kita-Daito Basin and KPR–Daito Ridge intersection, and this source melted due to rifting-induced decompression.

As plate subduction started along the nascent Izu-Bonin at c. 52 Ma (Figures 11 and 12; Ishizuka, Tani, et al., 2011) it is logical that this was the source of the arc signature in the 45–42 Ma Northern Philippine Sea volcanics. The occurrence of Eocene arc magmatism on the KPR has been identified based on the volcanoclastic deposits drilled in the rear arc side of the KPR (e.g., Ishizuka et al., 2018; Waldman et al., 2020). Accordingly it is possible to assume that the Northern Philippine Sea volcanics formed by rear arc magmatism behind the Izu-Bonin arc between 45 and 42 Ma. However, there are some observations which may not be consistent with this assumption. Westernmost Northern Philippine Sea volcanics are found in the western Kita-Daito Basin, which is now subducting along the Ryukyu Trench: a distance of around 450 km from the KPR. Since there is no clear evidence of significant extension in the direction perpendicular to the trend of KPR since Eocene, this distance can be regarded as a distance between the locus of the Eocene magmatism and the contemporaneous Izu-Bonin arc. By assuming a rate of plate convergence of up to several cm/year, it is very unlikely that the newly

subducting Pacific slab reached 450 km away from the arc front (Bonin Islands) within 3–4 m.y. (e.g., Ishizuka et al., 2020); the implication being that this slab would not have been able to supply slab-derived material to generate arc magmatism.

Comparison between the Northern Philippine Sea volcanics and other Eocene Izu-Bonin arc material highlights the difference between these volcanics. Eocene Hahajima Group rocks from the Izu-Bonin forearc, which are contemporaneous with the Northern Philippine Sea volcanics, share some isotopic characteristics with Northern Philippine Sea volcanics. That is, on Pb isotopic plots, they are plotted on or close to NHRL (Figures 8a–8c). However, the Northern Philippine Sea volcanics generally have higher $^{206}\text{Pb}/^{204}\text{Pb}$ (Figures 8a–8e). Younger Eocene - Oligocene KPR volcanics are distinct by having lower $^{206}\text{Pb}/^{204}\text{Pb}$, but higher $\Delta^{207}\text{Pb}/^{204}\text{Pb}$, $\Delta^{208}\text{Pb}/^{204}\text{Pb}$ and $^{143}\text{Nd}/^{144}\text{Nd}$ (Figures 8a–8e; Ishizuka, Taylor, et al., 2011). These observations seem to contradict the assumption that the Northern Philippine Sea volcanics correspond to rear-arc Izu-Bonin magmatism because slab-derived components for the Izu-Bonin arc are consistently more radiogenic in Pb and Sr isotopes than the sub-Philippine Sea mantle. Rear arc magmas with less slab-derived component are expected to have lower $^{206}\text{Pb}/^{204}\text{Pb}$, $\Delta^{207}\text{Pb}/^{204}\text{Pb}$ and $^{87}\text{Sr}/^{86}\text{Sr}$ (e.g., Taylor & Nesbitt, 1998; Hochstaedter et al., 2001; Ishizuka et al., 2003, 2011a, 2020) relative to the frontal arc magmas such as Bonin Islands and KPR.

Another observation which may not be consistent with the assumption that the Northern Philippine Sea volcanics are the product of Izu-Bonin arc magmatism is lack of geochemical variation with distance from the KPR. Trace element ratios indicative of contribution of slab-derived fluid/melt such as Ba/La and Th/LREE show no systematic spatial variation (Figure 10), which is striking contrast with younger Izu-Bonin arc with clear across-arc geochemical variation reflecting variation in abundance and composition of slab-derived material (e.g., Hochstaedter et al., 2001; Ishizuka et al., 2003; Taylor & Nesbitt, 1998). This implies that enrichment in fluid-mobile elements and Th in the Northern Philippine Sea volcanics was not caused by flux from subducting Pacific Plate beneath the Izu-Bonin arc. These observations seem to imply that the Northern Philippine Sea volcanics are not associated with subduction of Pacific Plate since Eocene, that is, have a separate magmatic origin to the Izu-Bonin arc.

Another possible subduction system which might have a link with the Northern Philippine Sea volcanics is the slab descending beneath the Philippine arc, that is, subduction from the opposite side of the Philippine Sea Plate to the Izu-Bonin arc. This arc established in the Mesozoic and was active until the Eocene (summarized in Deschamps & Lallemand, 2002). Even though the precise geographic relationship between the Daito Ridge Group and Philippine subduction in the Eocene is not clear, again the Northern Philippine Sea volcanics show no spatial geochemical variation indicating arc polarity (Figure 10). It is also difficult to explain the limited age range of the Northern Philippine Sea volcanics if the Philippine arc had been active since Mesozoic. It seems to be unlikely that any Eocene subduction system has a direct link to the activity of the Northern Philippine Sea volcanics.

Amami Seamounts in the Kita-Daito Basin are supposed to correspond to basaltic magma without the slab-derived component found in other rift basins such as the Mariana Trough as mentioned above. The origin of these basalts will be discussed further in the next section.

6.2. Origin of Basaltic Magmatism of the Amami Seamounts

Basalts from the Amami Seamounts show E-MORB-like geochemical characteristics without signature of slab-derived material and are geochemically clearly distinct from the Northern Philippine Sea volcanics. These basalts are also significantly younger (>3 m.y.) than the Northern Philippine Sea volcanics (Figure 12). The Amami Seamounts might represent a late stage of magmatism in the Kita-Daito Basin, that is, low degree melting of asthenospheric mantle associated with the final extension of the Kita-Daito Basin. This asthenospheric mantle clearly possesses Indian ocean MORB-type isotopic characteristics which is consistent with regional asthenospheric character of the Philippine Sea since Eocene.

It is recognized that localized basaltic magmatism can occur during continental rifting prior to seafloor spreading, like observed in the Main Ethiopian Rift (e.g., Ebinger & Casey, 2001). Localized magma input produces strips of mafic crust, but coherent ocean crust is not developed (e.g., Ebinger & Casey, 2001). The occurrence of the basalts in the Kita-Daito Basin seems to be somewhat similar to this setting. The difference, however, is

this basaltic magmatism appears to be the last magmatism in the Kita-Daito Basin rather than the earliest, that is, it is likely to correspond to the magmatism at the final stage of extension of the Kita-Daito Basin (Figure 11).

As a comparison of the well-observed magmatism at the waning stage of rift basin formation in the Philippine Sea area, post-spreading magmatism in the Shikoku Basin in the Philippine Sea formed elongated edifices at the extinct spreading center (Ishizuka et al., 2009). This magmatism had been active until 8 m.y. after the cessation of seafloor spreading. Long axes of the 37.5 Ma-Kanami Seamount and 35 Ma-Tete Seamount are ENE-WSE, which is oblique to the dominant E-W-trending seafloor fabric of the Kita-Daito Basin (Figure 1b). The location of the spreading center is not yet clear for this basin, however, if we assume N-S extension the locations of the basaltic seamounts have variable distances from the spreading center wherever it was. The difference in locus of magmatism between the Kinan Seamount Chain and the Amami Seamounts in the Kita-Daito Basin might be related to the contrasting origins of these basins. That is, while the Kita-Daito Basin did not evolve to spreading stage with production of ocean crust, the Shikoku Basin formed ocean crust at a clearly defined spreading center. Accordingly, the Kita-Daito Basin might only have had diffuse magmatism caused by decompression of unmetasomatized asthenospheric mantle, which were not geographically focused.

Since the Amami Seamount basalts are highly enriched in incompatible elements relative to the basalts from ocean crust in the Philippine Sea, it seems to correspond to low degree of melts with enriched portion of heterogeneous mantle. Isotopic characteristics of these basalts are similar to that of basalts from the Kinan Seamount Chain (Ishizuka et al., 2009), that is, EM1-like character, but clearly distinct from that of OIB-like basalts from oceanic plateaus (e.g., Urdaneta Plateau, Oki-Daito Rise) and seamounts in the Minami-Daito Basin and on the Oki-Daito Ridge, which are argued to be associated with “Oki-Daito plume” (Ishizuka et al., 2013) and show EM-2-like isotopic signature (Figure 8). In the Kinan Seamount Chain, it is interpreted that the enriched and most fusible component selectively melted at the waning final stage of the backarc basin spreading, possibly with weakened upwelling and lowering temperature beneath the spreading axis (Ishizuka et al., 2009). This interpretation might be applicable to the Amami Seamounts basalts. Since these enriched basalts are the youngest magmatic products in this basin, this basaltic magmatism occurred at the final stage of the rifting/spreading of the basin, with low degree of melting with larger contribution of enriched portion of the asthenospheric mantle. Major difference between the Shikoku Basin and the Kita-Daito Basin is that the Kita-Daito Basin appears to have never evolved to the seafloor spreading stage, but had only limited production of basaltic magma forming seamounts rather than ocean crust. This implies that a larger degree of melting of asthenospheric mantle, which produced N-MORB magma, might have not occurred in the Kita-Daito Basin. Late Eocene ages of these basalts might indicate that the formation of the Kita-Daito Basin continued until c. 37.5–33 Ma, and ceased (Figure 11).

This age is close to the end of main spreading stage of the West Philippine Basin (Figure 12; e.g., Sasaki et al., 2014). Spreading along the CBF Rift ceased progressively from southeast to northwest, between approximately 37.5 Ma at 133°E and 35.5 Ma at 130°E (Sasaki et al., 2014). Close timing between the possibly last stage of volcanism in the Kita-Daito Basin and end of main spreading of the West Philippine Basin seem to imply a tectonic link between the spreading of the two basins.

6.3. Origin of Indian and Pacific MORB-Type Signature

The Pb isotopic composition of the Northern Philippine Sea volcanics, clustered near NHRL on Pb-Pb isotopic plots, indicates a contribution of a Pacific MORB-type component to the source of the Northern Philippine Sea volcanics. Ce/Pb - $\Delta^{208}\text{Pb}/^{204}\text{Pb}$ plot indicates that the component with $\Delta^{208}\text{Pb}/^{204}\text{Pb}$ near 0 has very low Ce/Pb (Figure 9b). This suggests that the component with Pacific MORB Pb isotopes is material was enriched in fluid-mobile elements relative to the mantle, and is likely derived from subducting Pacific altered ocean crust.

Mantle metasomatized by this slab-derived component was involved in melt production not only for the Mesozoic arc, but also for Eocene Northern Philippine Sea volcanics and igneous rocks from the KPR–Daito Ridge intersection.

Currently available plate motion reconstructions do not define which plate was subducting at c. 120 Ma to generate the Mesozoic arc and the Eocene Daito Ridge Group. However, the Pacific MORB isotopic character of the subducting slab could provide a constraint on future tectonic reconstructions of Mesozoic Asia.

Isotopic characteristics of the original wedge mantle prior to the metasomatism in the Mesozoic is difficult to identify using the available data set. Since unmetasomatized mantle is expected to have Ce/Pb of 20–30, almost vertical trend of the Northern Philippine Sea volcanics on Ce/Pb - $\Delta^{208}\text{Pb}/^{204}\text{Pb}$ plot might imply that the asthenospheric mantle has $\Delta^{208}\text{Pb}/^{204}\text{Pb}$ of around 0, that is, Pacific MORB-like isotopic composition. However, further clarification requires more robust estimation using fluid-immobile element isotopes such as Hf.

On the other hand, Late Eocene Amami Seamounts basalts show enriched MORB-like composition with no contribution of slab-derived component. Accordingly, the basalts can be regarded as melt from asthenospheric mantle, that is, they possess isotopic characteristics of the mantle beneath the Kita-Daito Basin. These basalts show $\Delta^{207}\text{Pb}/^{204}\text{Pb}$ of 1.9–2.9 and $\Delta^{208}\text{Pb}/^{204}\text{Pb}$ of 42.2–49.6 with $^{206}\text{Pb}/^{204}\text{Pb}$ of 18.0–18.2, and this clearly indicates they have an Indian Ocean MORB-type asthenospheric source. This is consistent with the characteristics of other MORB-type basalts from ocean basins in the Philippine Sea such as the West Philippine Basin and Shikoku Basin. This may imply that the progress of rifting in the Kita-Daito Basin, accompanied by upwelling and decompression of asthenospheric mantle, finally allowed asthenospheric melt with Indian Ocean characteristics to erupt and form the Amami Seamounts.

6.4. Driving Force of Basin Formation and Magmatism -Interplay of Mantle Plume and Subduction-

Age range of the Northern Philippine Sea volcanics overlaps with the early stages of magmatism associated with Oki-Daito plume, which generated the oceanic plateaus such as Oki-Daito Rise and Urdaneta Plateau (Figures 11 and 12; Ishizuka et al., 2013). Causes of spreading in the Kita-Daito Basin is not yet clear. However, close timing between the onset of the magmatism in the Kita-Daito Basin and arrival of the Oki-Daito Plume beneath this region suggests the plume may have been a trigger for rifting.

The Northern Philippine Sea volcanics seem to be centered in the area surrounding the Oki-Daito Rise before formation of the Kita-Daito Basin. Klein and Kobayashi (1980) argued based on the results at DSDP Sites 445 and 446 that the recovery of reworked Nummulites indicates that the crest of the Daito Ridge was at or near sea level in middle-to late Eocene and has subsided about 1,500 m to its current depth. Daito Ridge Group exposes deep crustal section of arc origin consisting of volcanics, plutonics and schists (e.g., Mizuno et al., 1977; Hickey-Vargas, 2005; Ishizuka, Taylor, et al., 2011; Tani et al., 2012; this study), and even serpentinized peridotites from upper mantle (Morishita et al., 2018). The age of arc magmatism has been reported to be Jurassic and Cretaceous (c. 110–160 Ma; e.g., Hickey-Vargas, 2005; Ishizuka, Taylor, et al., 2011; Tani et al., 2012; this study). These rocks were found from the upper section of the ridges and also occur as clasts in conglomerates of shallow water origin recovered at Site 445 (Figures 1a and 1b; Klein & Kobayashi, 1980). Furthermore, amphiboles from the volcanoclastics from Site 445 as well as those from the sandstone recovered in the Amami Sankaku Basin at Site 1438E of IODP Exp. 351 (Figures 1a and 1b), show close ages to the Northern Philippine Sea volcanics. Geochemical signatures of these amphiboles imply that they are associated with magma with arc-like signature (Figure 12; Hickey-Vargas et al., 2013; Waldman et al., 2020). This seems to indicate that these amphiboles were derived from the Northern Philippine Sea Seamounts. This geological information from the Daito Ridge Group indicates that terrane including the Daito Ridge Group with some Northern Philippine Sea Seamounts on top was uplifted and subject to erosion before significant post-Eocene subsidence.

The geologic history summarized above indicates that the Daito Ridge Group crust experienced uplift in the Middle Eocene or before and then subsequent subsidence. Timing of the uplift is not clear. However, it could be associated with arrival of Oki-Daito plume which caused OIB-type magmatism initiated at around 50 Ma to form oceanic plateaus including Oki-Daito Rise and sills drilled at Site 446 in the Minami-Daito Basin (Hickey-Vargas, 1998; Ishizuka et al., 2013; Lallemand, 2016). Arrival of the plume might have caused domal uplift and localized rifting/spreading due to the small scale convection in the plume head (Baragar et al., 1996; Griffiths & Campbell, 1991). Subsequently flattening of the plume head, and increasing distance from the plume center and cooling of lithosphere might have caused subsidence of the Daito Ridge Group area after Eocene.

In terms of the temporal and causal relationship between volcanism and rifting generated by plume arrival, Hooper (1990) demonstrated by analysis of flow directions of flood basalts that in the cases of Deccan trap and Columbia River basalt, flood basalt magmatism preceded crustal extension in these areas. Hooper (1990) insisted based on this observation that arrival of mantle plume caused flood basalt volcanism and the plume acted as foci for continental rifting in a lithosphere under regional extensional strain. This scenario might be applicable to

the case of the regional extension including the formation of the Kita-Daito Basin. Rifting and limited seafloor spreading to form intervening basins in the Daito Ridge Group could have been triggered by the arrival of the Oki-Daito plume as discussed above (Figure 11). However, prolonged rifting/spreading in these basins probably requires interplay with other regional stress regime.

The volcanism which is thought to be associated with the Oki-Daito plume initiated at 50 Ma or earlier (Hickey-Vargas, 1998; Ishizuka et al., 2013). In this case, possible cause for the younger regional extension on the Philippine Sea Plate could be (a) backarc extension caused by subduction from the Philippine Trench, and (b) extension associated with subduction initiation of the Pacific Plate along the IBM arc margin (Figure 11).

Seafloor fabric of the Kita-Daito Basin implies north-south extension in the current geographic frame. Assumed axis of extension in this basin intersected KPR, that is, ancient IBM arc, at high angle. This situation implies that the extension of the Kita-Daito Basin is unlikely to have been associated with subduction along the incipient IBM arc margin, that is, unlikely to have taken place as backarc rifting/spreading of the IBM arc. Also by 45 Ma, subduction along the IBM arc had been stabilized, and volcanic arc was established (e.g., Ishizuka et al., 2020). It does not seem to have tectonic event in this period along this arc to cause rifting in the direction intersecting the arc with high angle in its rear arc area.

Another tectonic process which might be related to the extension and opening of the Kita-Daito Basin is subduction along the paleo-Philippine arc (Deschamps & Lallemand, 2002; Figure 11). Deschamps and Lallemand (2002) proposed that the West Philippine Basin started opening in the back of Philippine arc. Compilation of ages of arc magmatism in the eastern Philippine (Deschamps & Lallemand, 2002; Zahirovic et al., 2014) shows that the paleo-Philippine arc volcanism had been active since Cretaceous to c. 40 Ma. This observation raises the possibility that the subduction along the paleo-Philippine arc might have caused extension in its backarc side, and maintained rifting/spreading in the Daito Ridge Group in middle to late Eocene. Timing of formation of the Kita-Daito Basin estimated from the age of volcanism appears to have been largely consistent with the active period of the paleo-Philippine arc. However, the precise geographic relations between the Kita-Daito Basin and the Philippine arc subduction zone in Eocene time is not clear, which makes difficult to test this hypothesis.

Other than subduction, another process to cause rifting of the Kita-Daito Basin could be that the effect of spreading and changing attitude of the West Philippine Basin has some causal link with rifting/spreading of the Kita-Daito Basin. The main opening stage of the West Philippine Basin is thought to be around 55-50 Ma and 35 Ma (e.g., Deschamps & Lallemand, 2002; Sasaki et al., 2014). This period overlaps with that of the volcanism of the Northern Philippine Sea volcanics, which is envisaged as being associated with rifting/opening of the Kita-Daito basin (Figure 11). After middle Eocene, the spreading axis of the West Philippine Basin is proposed to have jumped to a new axis position (Deschamps & Lallemand, 2002). The driver for this shift in spreading could have been the retreat of the newly born IBM trench as well as the upwelling of the Oki-Daito plume. In this scenario, the northern margin of the West Philippine Basin (which corresponds to the area where Northern Philippine Sea Seamounts and the Kita-Daito Basin formed in the Mesozoic terrane; Figures 1c and 11), could have also been under similar extension, or potentially the effects of the reorganization of West Philippine Basin spreading which potentially caused extension and transtension in the surrounding area. To test this hypothesis, origin and age of tectonic features along northern and southernmost margin of the West Philippine Basin needs to be examined alongside a better understanding of the relative motion among the terranes within the Philippine Sea Plate.

7. Conclusions

Recent investigation in the northern part of the Philippine Sea Plate has revealed some crucial information to reconstruct tectonic setting and understand magmatism during the period when the IBM arc formed by subduction initiation of the Pacific Plate beneath the Philippine Sea Plate.

1. Eocene andesitic magmatism (Northern Philippine Sea volcanics) has been discovered in and around the Kita-Daito Basin. Ar/Ar and zircon U-Pb dating results of these igneous rocks indicate that the andesitic rocks formed mainly between 45 and 42 Ma.
2. These andesitic rocks show enrichment in fluid-mobile elements and Th, and have depletion in HFSE. This implies that the source of the Northern Philippine Sea volcanics has contribution of slab-derived material.

3. Lack of any systematic spatial variation of the slab component in the Northern Philippine Sea volcanics as well as great distance (over 400 km) from the arc front make unlikely that the Northern Philippine Sea volcanics is associated with contemporaneous subduction either along the Izu-Bonin arc or Philippine arc.
4. The Northern Philippine Sea volcanics share geochemical characteristics with Eocene igneous rocks from the KPR–Daito Ridge intersection. This implies that a similar component contributes to their magmatism. Considering that both regions once belong to the Daito Ridge Group terrane, this component is likely to be lithospheric mantle underlying Mesozoic remnant arc of the Daito Ridge Group. This mantle was previously metasomatized by slab-derived component during Mesozoic subduction.
5. The Mesozoic subduction component is likely to be fluid mainly from subducting altered ocean crust with Pacific MORB isotopic characteristics.
6. Basalt recovered from the Amami Seamounts shows E-MORB-like geochemical characteristics without a signature of slab-derived material. These basalts are younger than andesites in this region (37.5–33 Ma), and might mark late-stage magmatism from low-degree asthenospheric melting beneath the Kita-Daito Basin. This asthenospheric mantle clearly possesses Indian ocean MORB-type isotopic characteristics, which are consistent with the regional character of the Philippine Sea since Eocene.
7. Even though the cause of Kita-Daito Basin spreading is not yet clear, close timing between the onset of the magmatism in the Kita-Daito Basin and the arrival of the Oki-Daito Plume implies a causal link.
8. The results of this study indicate that the Kita-Daito Basin postdates the initiation of subduction of the Pacific Plate along the IBM arc.

Data Availability Statement

All data generated in this study are included in the Supporting Information and can be found in the Mendeley database (<https://doi.org/10.17632/nvhb6yyg9p.1>).

Acknowledgments

Part of this study was conducted under the project entitled Basic Researches on Exploration Technologies for Deep Sea Natural Resources, which is commissioned to JOGMEC by METI. We thank METI for approving publication of the data. We thank the officers, crews, and onboard scientists of the R/V *Hakurei-maru No. 2*, R/V *Yokosuka*, R/V *Hakuho maru* and R/V *Shinsei maru*, and submersible pilots of *Shinkai 6500*. We would like to thank K. Yamanobe for preparation of glass beads and assistance with the ICP-MS measurements. We appreciate A. Owada, T. Sato and E. Hirabayashi for preparation of thin sections. We also thank T. Sasaki, T. Shimono, A. Tokumoto, and H. Nagato for helping preparation of rock powder, and N. Geshi and Y. Ishizuka for the maintenance of XRF at GSJ-lab. We appreciate M. Narui and M. Yamazaki at IMR, Tohoku University, and Oregon State University for neutron irradiation. We would like to thank R. Okumura, H. Yoshinaga, Y. Iinuma for irradiation of dated samples at KUR, Institute for Integrated Radiation and Nuclear Science, Kyoto University. This work was supported by JSPS KAKENHI Grant Nos. JP17K05686, JP25287133, and JP21H01183, and JSPS bilateral grant (Japan-UK) for OI. The authors acknowledge the constructive reviews by Michael Bizimis, Maryjo Brounce, and 2 anonymous reviewers and helpful editorial comments by Janne Blüchert-Toft.

References

- Arculus, R. J., Ishizuka, O., Bogus, K. A., Gurnis, M., Hickey-Vargas, R., Aljehdali, M. H., et al. (2015). A record of spontaneous subduction initiation in the Izu–Bonin–Mariana arc. *Nature Geoscience*, 8(9), 728–733. <https://doi.org/10.1038/NGEO2515>
- Baragar, W. R. A., Ernst, R. E., Hulbert, L., & Peterson, T. (1996). Longitudinal petrochemical variation in the Mackenzie dyke swarm, north-western Canadian shield. *Journal of Petrology*, 37(2), 317–359. <https://doi.org/10.1093/ptrology/37.2.317>
- Black, L. P., Kamo, S. L., Allen, C. M., Davis, D. W., Aleinikoff, J. N., Valley, J. W., et al. (2004). Improved $^{206}\text{Pb}/^{238}\text{U}$ microprobe geochronology by the monitoring of a trace-element-related matrix effect; SHRIMP, ID-TIMS, ELA-ICP-MS and oxygen isotope documentation for a series of zircon standards. *Chemical Geology*, 205(1–2), 115–140. <https://doi.org/10.1016/j.chemgeo.2004.01.003>
- Brandl, P. A., Hamada, M., Arculus, R. J., Johnson, K., Marsaglia, K. M., Ishizuka, O., et al. (2017). The arc arises: The links between volcanic output, arc evolution, and melt composition. *Earth and Planetary Science Letters*, 461, 73–84. <https://doi.org/10.1016/j.epsl.2016.12.027>
- Deschamps, A., & Lallemand, S. (2002). The West Philippine Basin: An Eocene to early Oligocene back arc basin opened between two opposed subduction zones. *Journal of Geophysical Research*, 107(B12), 2322. <https://doi.org/10.1029/2001JB001706>
- Ebinger, C. J., & Casey, M. (2001). Continental breakup in magmatic provinces: An Ethiopian example. *Geology*, 29(6), 527–530. [https://doi.org/10.1130/0091-7613\(2001\)029<0527:CBIMPA>2.0.CO;2](https://doi.org/10.1130/0091-7613(2001)029<0527:CBIMPA>2.0.CO;2)
- Fleck, R. J., Sutter, J. F., & Elliot, D. H. (1977). Interpretation of discordant $^{40}\text{Ar}/^{39}\text{Ar}$ age-spectra of Mesozoic tholeiites from Antarctica. *Geochimica et Cosmochimica Acta*, 41(1), 15–32. [https://doi.org/10.1016/0016-7037\(77\)90184-3](https://doi.org/10.1016/0016-7037(77)90184-3)
- Gerya, T., Stern, R. J., Baes, M., Sobolev, S., & Whattam, S. (2015). Plume-induced subduction initiation triggered plate tectonics on Earth. *Nature*, 527(7577), 221–225. <https://doi.org/10.1038/nature15752>
- Griffiths, R. W., & Campbell, I. H. (1991). Interaction of mantle plume heads with the Earth's surface and onset of small-scale convection. *Journal of Geophysical Research*, 96(B11), 18295–18310. <https://doi.org/10.1029/91jb01897>
- Hall, R. (2002). Cenozoic geological and plate tectonic evolution of SE Asia and the SW Pacific: Computer-based reconstructions and animations. *Journal of Asian Earth Sciences*, 20(4), 353–431. [https://doi.org/10.1016/S1367-9120\(01\)00069-4](https://doi.org/10.1016/S1367-9120(01)00069-4)
- Hart, S. R. (1984). A large-scale isotopic anomaly in the Southern hemisphere mantle. *Nature*, 309(5971), 753–757. <https://doi.org/10.1038/309753a0>
- Hickey-Vargas, R. (1991). Isotope characteristics of submarine lavas from the Philippine Sea: Implications for the origin of arc and basin magmas of the Philippine tectonic plate. *Earth and Planetary Science Letters*, 107(2), 290–304. [https://doi.org/10.1016/0012-821x\(91\)90077-u](https://doi.org/10.1016/0012-821x(91)90077-u)
- Hickey-Vargas, R. (1998). Origin of the Indian Ocean-type isotopic signature in basalts from Philippine Sea plate spreading centers: An assessment of local versus large-scale processes. *Journal of Geophysical Research: Solid Earth*, 103(B9), 20963–20979. <https://doi.org/10.1029/98jb02052>
- Hickey-Vargas, R. (2005). Basalt and tonalite from the Amami plateau, northern West Philippine basin: New early cretaceous ages and geochemical results, and their petrologic and tectonic implications. *Island Arc*, 14(4), 653–665. <https://doi.org/10.1111/j.1440-1738.2005.00474.x>
- Hickey-Vargas, R., Ishizuka, O., & Bizimis, M. (2013). Age and geochemistry of volcanic clasts from DSDP Site 445, Daito Ridge and relationship to Minami-Daito Basin and early Izu-Bonin arc magmatism. *Journal of Asian Earth Sciences*, 70–71, 193–208. <https://doi.org/10.1016/j.jseas.2013.03.013>
- Hickey-Vargas, R., Yagodinski, G. M., Ishizuka, O., McCarthy, A., Bizimis, M., Kusano, Y., et al. (2018). Origin of depleted basalts during subduction initiation and early development of the Izu-Bonin-Mariana Island arc: Evidence from IODP expedition 351 site U1438, Amami-Sankaku Basin. *Geochimica et Cosmochimica Acta*, 229, 85–111. <https://doi.org/10.1016/j.gca.2018.03.007>

- Hochstaedter, A. G., Gill, J. B., & Morris, J. D. (1990). Volcanism in the Sumisu Rift, II, subduction and non-subduction related components. *Earth and Planetary Science Letters*, 100(1–3), 195–209. [https://doi.org/10.1016/0012-821x\(90\)90185-z](https://doi.org/10.1016/0012-821x(90)90185-z)
- Hochstaedter, A. G., Gill, J. B., Peters, R., Broughton, P., Holden, P., & Taylor, B. (2001). Across-arc geochemical trends in the Izu-Bonin arc: Contributions from the subducting slab. *Geochemistry, Geophysics, Geosystems*, 2(7), 2000GC000105. <https://doi.org/10.1029/2000gc000105>
- Hooper, P. R. (1990). The timing of crustal extension and the eruption of continental flood basalts. *Nature*, 345(6272), 246–249. <https://doi.org/10.1038/345246a0>
- Ishizuka, O., Hickey-Vargas, R., Arculus, R. J., Yogodzinski, G. M., Savov, I. P., Kusano, Y., et al. (2018). Age of Izu-Bonin-Mariana arc basement. *Earth and Planetary Science Letters*, 481, 80–90. <https://doi.org/10.1016/j.epsl.2017.10.023>
- Ishizuka, O., Tani, K., Reagan, M. K., Kanayama, K., Umino, S., Harigane, Y., et al. (2011). The timescales of subduction initiation and subsequent evolution of an oceanic island arc. *Earth and Planetary Science Letters*, 306(3–4), 229–240. <https://doi.org/10.1016/j.epsl.2011.04.006>
- Ishizuka, O., Taylor, R. N., Milton, J. A., & Nesbitt, R. W. (2003). Fluid-mantle interaction in an intra-oceanic arc: Constraints from high-precision Pb isotopes. *Earth and Planetary Science Letters*, 211(3–4), 221–236. [https://doi.org/10.1016/s0012-821x\(03\)00201-2](https://doi.org/10.1016/s0012-821x(03)00201-2)
- Ishizuka, O., Taylor, R. N., Ohara, Y., & Yuasa, M. (2013). Upwelling, rifting and age-progressive magmatism from the Oki-Daito mantle plume. *Geology*, 41(9), 1011–1014. <https://doi.org/10.1130/G34525.1>
- Ishizuka, O., Taylor, R. N., Umino, S., & Kanayama, K. (2020). Geochemical evolution of arc and slab following subduction initiation: A record from the Bonin Islands, Japan. *Journal of Petrology*, 61(5). <https://doi.org/10.1093/ptrology/egaa050>
- Ishizuka, O., Taylor, R. N., Yuasa, M., & Ohara, Y. (2011). Making and breaking an island arc: A new perspective from the Oligocene Kyushu–Palau arc, Philip-pine Sea. *Geochemistry, Geophysics, Geosystems*, 12(5), Q05005. <https://doi.org/10.1029/2010GC003440>
- Ishizuka, O., Uto, K., Yuasa, M., & Hochstaedter, A. G. (2002). Volcanism in the earliest stage of back-arc rifting in the Izu-Bonin arc revealed by laser-heating ⁴⁰Ar/³⁹Ar dating. *Journal of Volcanology and Geothermal Research*, 120(1–2), 71–85. [https://doi.org/10.1016/s0377-0273\(02\)00365-7](https://doi.org/10.1016/s0377-0273(02)00365-7)
- Ishizuka, O., Yuasa, M., Tamura, Y., Shukuno, H., Stern, R. J., Naka, J., et al. (2010). Migrating shoshonitic magmatism tracks Izu-Bonin-Mariana intra-oceanic arc rift propagation. *Earth and Planetary Science Letters*, 294(1–2), 111–122. <https://doi.org/10.1016/j.epsl.2010.03.016>
- Ishizuka, O., Yuasa, M., Taylor, R. N., & Sakamoto, I. (2009). Two contrasting magmatic types coexist after the cessation of back-arc spreading. *Chemical Geology*, 266(3–4), 283–305. <https://doi.org/10.1016/j.chemgeo.2009.06.014>
- Iwano, H., Orihashi, Y., Hirata, T., Ogasawara, M., Danhara, T., Horie, K., et al. (2013). An inter-laboratory evaluation of OD-3 zircon for use as a secondary U-Pb dating standard. *Island Arc*, 22(3), 382–394. <https://doi.org/10.1111/iar.12038>
- Johnson, C. M., & Beard, B. L. (1999). Correction of instrumentally produced mass fractionation during isotopic analysis of Fe by thermal ionization mass spectrometry. *International Journal of Mass Spectrometry*, 193(1), 87–99. [https://doi.org/10.1016/s1387-3806\(99\)00158-x](https://doi.org/10.1016/s1387-3806(99)00158-x)
- Johnson, K. E., Marsaglia, K. M., Brandl, P. A., Barth, A., Waldman, R. J., Ishizuka, O., et al. (2021). Intra-oceanic submarine arc evolution recorded in an ~1-km-thick rear-arc succession of distal volcanoclastic lobe deposits. *Geosphere*, 17(4), 957–980. <https://doi.org/10.1130/GES02321.1>
- Kanayama, K., Umino, S., & Ishizuka, O. (2012). Eocene volcanism during the incipient stage of Izu–Ogasawara arc: Geology and petrology of the mukojima Island group, the Ogasawara Islands. *Island Arc*, 21(4), 288–316. <https://doi.org/10.1111/iar.12000>
- Kanayama, K., Umino, S., & Ishizuka, O. (2014). Shallow submarine volcano group in the early stage of island arc development: Geology and petrology of small islands south off Hahajima main island, the Ogasawara Islands. *Journal of Asian Earth Sciences*, 85, 1–25. <https://doi.org/10.1016/j.jseaes.2014.01.012>
- Karig, D. (1975). Basin Genesis in the Philippine Sea. *Initial Reports of the Deep Sea Drilling Project*, 31, 857–879. <https://doi.org/10.2973/dsdp.proc.31.142.1975>
- Kasuga, S., Koyama, K., & Kaneko, Y. (1986). Geomagnetic and gravity anomalies around the Daito Ridge. *Report of Hydrographic Researches*, 21, 65–76. (Japanese with English abstract).
- Kelley, K. A., Plank, T., Ludden, J., & Staudigel, H. (2003). Composition of altered oceanic crust at ODP Sites 801 and 1149. *Geochemistry, Geophysics, Geosystems*, 4(6). <https://doi.org/10.1029/2002GC000435>
- Klein, G. V., & Kobayashi, K. (1980). Geological summary of the North Philippine Sea, based on Deep Sea drilling project Leg 58 results. *Initial Reports of the Deep Sea Drilling Project*, 58, 951–961. U.S. Government Printing Office, Washington, D.C..
- Lallemand, S. (2016). Philippine Sea Plate inception, evolution, and consumption with special emphasis on the early stages of Izu-Bonin-Mariana subduction. *Progress in Earth and Planetary Science*, 3(1), 15. <https://doi.org/10.1186/s40645-016-0085-6>
- Le Maitre, R. W. (Ed.). (1989). *A classification of igneous rocks and glossary of terms*. Blackwell.
- Leng, W., & Gurnis, M. (2015). Subduction initiation at relic arcs. *Geophysical Research Letters*, 42(17), 7014–7021. <https://doi.org/10.1002/2015GL064985>
- Li, H.-Y., Taylor, R. N., Prytulak, J., Kirchenbaur, M., Shervais, J. W., Ryan, J. G., et al. (2019). Radiogenic isotopes document the start of subduction in the Western Pacific. *Earth and Planetary Science Letters*, 518, 197–210. <https://doi.org/10.1016/j.epsl.2019.04.041>
- Lukács, R., Harangi, S., Bachmann, O., Guillong, M., Danišik, M., Buret, Y., et al. (2015). Zircon geochronology and geochemistry to constrain the youngest eruption events and magma evolution of the Mid-Miocene ignimbrite flare-up in the Pannonian Basin, eastern central Europe. *Contributions to Mineralogy and Petrology*, 170(5–6), 52. <https://doi.org/10.1007/s00410-015-1206-8>
- Macpherson, C., Dreher, S. T., & Thirlwall, M. F. (2006). Adakites without slab melting: High pressure differentiation of island arc magma, Mindanao, the Philippines. *Earth and Planetary Science Letters*, 243(3–4), 581–593. <https://doi.org/10.1016/j.epsl.2005.12.034>
- Matsuda, J., Saito, K., & Zasu, S. (1975). K–Ar age and Sr isotope ratio of the rocks in the manganese nodules obtained from the Amami Plateau, Western Philippine Sea. *Symposium on Geological Problems of the Philippine Sea*. (pp. 99–101). Geological Society of Japan.
- McCarthy, A., Yogodzinski, G. M., Bizimis, M., Hickey-Vargas, R., Savov, I. P., Arculus, R., & Ishizuka, O. (2021). Volcanoclastic sandstones record the influence of subducted Pacific MORB on magmatism at the early Izu-Bonin arc. *Geochimica et Cosmochimica Acta*, 296, 170–188. <https://doi.org/10.1016/j.gca.2021.01.006>
- Mizuno, A., Okuda, Y., Nagumo, S., Kagami, H., & Nasu, N. (1978). *Subsidence of the Daito Ridge and Associated Basins, North Philippine Sea* (Vol. 29, pp. 239–243). American Association of Petroleum Geologists Memoir.
- Mizuno, A., Okuda, Y., Tamaki, K., Kinoshita, Y., Nohara, M., Yuasa, M., et al. (1975). Marine geology and geologic history of the Daito ridges area, Northwestern Philippine Sea (1). *Marine Science Monthly*, 7, 484–491. (in Japanese with English abstract).
- Mizuno, A., Shiki, T., & Aoki, H. (1977). Dredged rock and piston and gravity core data from the Daito ridges and the Kyushu-Palau Ridge in the North Philippine Sea. *Geological Studies of Ryukyu Islands*, 2, 107–119.
- Morishita, T., Tani, K., Soda, Y., Tamura, A., Mizukami, T., & Ghosh, B. (2018). The uppermost mantle section below a remnant proto-Philippine Sea island arc: Insights from the peridotite fragments from the Daito Ridge. *American Mineralogist*, 103(7), 1151–1160. <https://doi.org/10.2138/am-2018-6030>

- Nishizawa, A., Kaneda, K., Katagiri, Y., & Oikawa, M. (2014). Wide-angle refraction experiments in the Daito Ridges region at the northwestern end of the Philippine Sea plate. *Earth Planets and Space*, 66(1), 25. <https://doi.org/10.1186/1880-5981-66-25>
- Nishizawa, A., Kaneda, K., Katagiri, Y., & Oikawa, M. (2016). Crust and uppermost mantle structure of the Kyushu-Palau Ridge, remnant arc on the Philippine Sea plate. *Earth Planets and Space*, 68(1), 30. <https://doi.org/10.1186/s40623-016-0407-3>
- Nishizawa, A., Kaneda, K., & Oikawa, M. (2011). Backarc basin oceanic crust and uppermost mantle seismic velocity structure of the Shikoku Basin, south of Japan. *Earth Planets and Space*, 63(2), 151–155. <https://doi.org/10.5047/eps.2010.12.003>
- Okino, K. (2015). Magnetic anomalies in the Philippine Sea: Implications for regional tectonics. *Journal of Geography*, 124, 729–747. (in Japanese). <https://doi.org/10.5026/jgeography.124.0000>
- Pearce, J. A., Stern, R. J., Bloomer, S. H., & Fryer, P. (2005). Geochemical mapping of the Mariana arc-basin system: Implications for the nature and distribution of subduction components. *Geochemistry, Geophysics, Geosystems*, 6(7), Q07006. <https://doi.org/10.1029/2004GC000895>
- Plank, T., Kelley, K. A., Murray, R. W., & Stern, L. Q. (2007). Chemical composition of sediments subducting at the Izu-Bonin trench. *Geochemistry, Geophysics, Geosystems*, 8(4), Q04H16. <https://doi.org/10.1029/2006GC001444>
- Reagan, M. K., Heaton, D. E., Schmitz, M. D., Pearce, J. A., Shervais, J. W., & Koppers, A. A. P. (2019). Forearc ages reveal extensive shortlived and rapid seafloor spreading following subduction initiation. *Earth and Planetary Science Letters*, 506, 520–529. <https://doi.org/10.1016/j.epsl.2018.11.020>
- Reagan, M. K., Ishizuka, O., Stern, R. J., Kelley, K. A., Ohara, Y., Blichert-Toft, J., et al. (2010). Fore-arc basalts and subduction initiation in the Izu-Bonin-Mariana system. *Geochemistry, Geophysics, Geosystems*, 11(3), Q03X12. <https://doi.org/10.1029/2009GC002871>
- Rickwood, P. C. (1989). Boundary lines within petrologic diagrams which use oxides of major and minor elements. *Lithos*, 22(4), 247–263. [https://doi.org/10.1016/0024-4937\(89\)90028-5](https://doi.org/10.1016/0024-4937(89)90028-5)
- Sasaki, T., Yamazaki, T., & Ishizuka, O. (2014). A revised spreading model of the West Philippine Basin. *Earth Planets and Space*, 66(1), 83. <https://doi.org/10.1186/1880-5981-66-83>
- Savov, I. P., Hickey-Vargas, R., D'Antonio, M., Ryan, J. G., & Spadea, P. (2006). Petrology and geochemistry of West Philippine Basin basalts and early Palau-Kyushu arc volcanic clasts from ODP Leg 195, site 1201D: Implications for the early history of the Izu-Bonin-Mariana arc. *Journal of Petrology*, 47(2), 277–299. <https://doi.org/10.1093/petrology/egi075>
- Shiki, T., Mizuno, A., & Kobayashi, K. (1985). Data listing of the bottom materials dredged and cored from the northern Philippine Sea. In T. Shiki (Ed.), *Geology of the northern Philippine Sea* (pp. 23–41). Tokai University Press.
- Shinjo, R., Chung, S.-L., Kato, Y., & Kimura, M. (1999). Geochemical and Sr–Nd isotopic characteristics of volcanic rocks from the Okinawa Trough and Ryukyu arc: Implications for the evolution of a young, intracontinental back arc basin. *Journal of Geophysical Research*, 104, 10591–10608. <https://doi.org/10.1029/1999JB900040>
- Stacey, J. S., & Kramers, J. D. (1975). Approximation of terrestrial lead isotope evolution by a two stage model. *Earth and Planetary Science Letters*, 26(2), 207–221. [https://doi.org/10.1016/0012-821x\(75\)90088-6](https://doi.org/10.1016/0012-821x(75)90088-6)
- Steiger, R. H., & Jäger, E. (1977). Subcommittee on geochronology: Convention on the use of decay constants in geo- and cosmochronology. *Earth and Planetary Science Letters*, 36(3), 359–362. [https://doi.org/10.1016/0012-821x\(77\)90060-7](https://doi.org/10.1016/0012-821x(77)90060-7)
- Stern, R. J. (2004). Subduction initiation: Spontaneous and induced. *Earth and Planetary Science Letters*, 226(3–4), 275–292. [https://doi.org/10.1016/s0012-821x\(04\)00498-4](https://doi.org/10.1016/s0012-821x(04)00498-4)
- Sun, S.-S., & McDonough, W. F. (1989). Chemical and isotopic systematics of oceanic basalts: Implications for mantle compositions and processes. In A. D. Saunders & M. J. Norry (Eds.), *Magmatism in the ocean basins* (Vol. 42, pp. 313–345). Geological Society Special Publication.
- Tanaka, T., Togashi, S., Kamioka, H., Amakawa, H., Kagami, H., Hamamoto, T., et al. (2000). JNdi-1: A neodymium isotopic reference in consistency with LaJolla neodymium. *Chemical Geology*, 168(3–4), 279–281. [https://doi.org/10.1016/s0009-2541\(00\)00198-4](https://doi.org/10.1016/s0009-2541(00)00198-4)
- Tani, K., Ishizuka, O., Ueda, H., Shukuno, H., Hirahara, Y., Nichols, A. R. L., et al. (2012). *Izu-Bonin arc: Intra-oceanic from the beginning? Unraveling the crustal structure of the Mesozoic proto-Philippine Sea plate*. AGU. Abstract in AGU Fall Meeting 2012.
- Taylor, R. N., Ishizuka, O., Michalik, A., Milton, J. A., & Croudace, I. W. (2015). Evaluating the precision of Pb isotope measurement by mass spectrometry. *Journal of Analytical Atomic Spectrometry*, 30(1), 198–213. <https://doi.org/10.1039/c4ja00279b>
- Taylor, R. N., & Nesbitt, R. W. (1998). Isotopic characteristics of subduction fluids in an intra-oceanic setting, Izu-Bonin Arc, Japan. *Earth and Planetary Science Letters*, 164(1–2), 79–98. [https://doi.org/10.1016/s0012-821x\(98\)00182-4](https://doi.org/10.1016/s0012-821x(98)00182-4)
- Thirlwall, M. E. (1991). Long-term reproducibility of multicollector Sr and Nd isotope ratio analysis. *Chemical Geology (Isotope Geoscience Section)*, 94(2), 85–104. [https://doi.org/10.1016/s0009-2541\(10\)80021-x](https://doi.org/10.1016/s0009-2541(10)80021-x)
- Tsutsumi, Y., Horie, K., Sano, T., Miyawaki, R., Momma, K., Matsubara, S., et al. (2012). LA-ICP-MS and SHRIMP ages of zircons in chevkinite and monazite tuffs from the Boso Peninsula, Central Japan. *Bulletin of the National Museum of Nature and Science, Series C*, 38, 15–32.
- Uchiumi, S., & Shibata, K. (1980). Errors in K–Ar age determination. *Bulletin of the Geological Survey of Japan*, 31, 267–273. (in Japanese with English abstract).
- van Hinsbergen, D. J. J., Steinberger, B., Guilmette, C., Maffione, M., Gürer, D., Peters, K., et al. (2021). A record of plume induced plate rotation triggering subduction initiation. *Nature Geoscience*, 14(8), 626–630. <https://doi.org/10.1038/s41561-021-00780-7>
- Vermeesch, P. (2018). IsoplotR: A free and open toolbox for geochronology. *Geoscience Frontiers*, 9(5), 1479–1493. <https://doi.org/10.1016/j.gsf.2018.04.001>
- Waldman, R. J., Marsaglia, K. M., Hickey-Vargas, R., Ishizuka, O., Johnson, K. E., McCarthy, A., et al. (2020). *Sedimentary and volcanic record of the nascent IBM arc from IODP site U1438*. Geological Society of America Bulletin. <https://doi.org/10.1130/B35612.1>
- Whattam, S., & Stern, R. J. (2015). Late cretaceous plume-induced subduction initiation along the southern and eastern margins of the caribbean: The first documented example with implications for the onset of plate tectonics. *Gondwana Research*, 27(1), 38–63. <https://doi.org/10.1016/j.gr.2014.07.011>
- Williams, I. S. (1998). U–Th–Pb geochronology by ion microprobe. In M. A. McKibben, W. C. P. Shanks, & W. I. Ridley (Eds.), *Applications of microanalytical techniques to understanding mineralizing processes* (Vol. 7, pp. 1–35). Reviews in Economic Geology.
- Yogodzinski, G., Bizimis, M., Hickey-Vargas, R., McCarthy, A., Hocking, B. D., Savov, I. P., et al. (2018). Implications of eocene-age Philippine Sea and forearc basalts for initiation and early history of the Izu-Bonin-Mariana arc. *Geochimica et Cosmochimica Acta*, 228, 136–156. <https://doi.org/10.1016/j.gca.2018.02.047>
- York, D. (1969). Least squares fitting of a straight line with correlated errors. *Earth and Planetary Science Letters*, 5, 320–324. [https://doi.org/10.1016/s0012-821x\(68\)80059-7](https://doi.org/10.1016/s0012-821x(68)80059-7)
- Yuasa, M., & Watanabe, T. (1977). Pre-cenozoic metamorphic rocks from the Daito Ridge in the northern Philippine Sea. *Japanese Association of Mineralogists, and Economic Geologists Journal*, 72(6), 241–251. <https://doi.org/10.2465/ganko1941.72.241>
- Zahirovic, S., Seton, M., & Müller, R. D. (2014). The cretaceous and cenozoic tectonic evolution of southeast Asia. *Solid Earth*, 5(1), 227–273. <https://doi.org/10.5194/se-5-227-2014>

Reference From the Supporting Information

Hauff, F., Hoernle, K., & Schmidt, A. (2003). Sr–Nd–Pb composition of mesozoic Pacific oceanic crust (site 1149 and 801, ODP Leg 185): Implications for alteration of ocean crust and the input into the Izu-Bonin-Mariana subduction system. *Geochemistry, Geophysics, Geosystems*, 4(8), 8913. <https://doi.org/10.1029/2002GC000421>